ACADÉMIE
DES SCIENCES
INSTITUT DE FRANCE

Comptes Rendus
Physique

Hung The Diep

Frustrated spin systems: history of the emergence of a modern physics

Volume 26 (2025), p. 225-251

Online since: 12 February 2025

https://doi.org/10.5802/crphys.235

The Comptes Rendus. Physique *are a member of the Mersenne Center for open scientific publishing*
www.centre-mersenne.org — e-ISSN : 1878-1535

ACADÉMIE DES SCIENCES
INSTITUT DE FRANCE

Comptes Rendus. Physique
2025, Vol. 26, p. 225-251
https://doi.org/10.5802/crphys.235

Review article / *Article de synthèse*

Frustrated spin systems: history of the emergence of a modern physics

Systèmes de spins frustrés : émergence d'une physique moderne

Hung The Diep [a]

[a] Laboratoire de Physique Théorique et Modélisation, CY Cergy Paris Université, CNRS, UMR 8089, 2 Avenue Adolphe Chauvin, 95302 Cergy-Pontoise Cedex, France
E-mail: diep@cyu.fr

Abstract. In 1977, Gérard Toulouse has proposed a new concept termed as "frustration" in spin systems. Using this definition, several frustrated models have been created and studied, among them we can mention the Villain's model, the fully frustrated simple cubic lattice, the antiferromagnetic triangular lattice. The former models are systems with mixed ferromagnetic and antiferromagnetic bonds, while in the latter containing only an antiferromagnetic interaction, the frustration is caused by the lattice geometry. These frustrated spin systems have novel properties that we will review in this paper. One of the striking aspects is the fact that well-established methods such as the renormalization group fail to deal with the nature of the phase transition in frustrated systems. Investigations of properties of frustrated spin systems have been intensive since the 80's. I myself got involved in several investigations of frustrated spin systems soon after my PhD. I have learned a lot from numerous discussions with Gérard Toulouse. Until today, I am still working on frustrated systems such as skyrmions. In this review, I trace back a number of my works over the years on frustrated spin systems going from exactly solved 2D Ising frustrated models, to XY and Heisenberg 2D and 3D frustrated lattices. At the end I present my latest results on skyrmions resulting from the frustration caused by the competition between the exchange interaction and the Dzyaloshinskii–Moriya interaction under an applied magnetic field. A quantum spin-wave theory using the Green's function method is shown and discussed.

Résumé. En 1977, Gérard Toulouse a introduit le concept nommé « frustration » pour les systèmes de spins dans lesquels une partie des interactions n'est pas satisfaite (cas de spins Ising) ou toutes les interactions ne sont pas satisfaites (cas de spins XY et Heisenberg). En utilisant cette notion, beaucoup de systèmes de spins frustrés ont été créés et étudiés. On peut mentionner quelques modèles populaires : le modèle de Villain, le modèle frustré sur un réseau cubique simple et le modèle antiferromagnétque sur un réseau triangulaire. La frustration dans les deux premiers modèles est due à un mélange des interactions ferromagnétiques et antiferromagnétiques, tandis que la frustration dans le dernier modèle est due à l'incompatibilité de l'interaction avec la géométrie du réseau (on dit alors « frustration par géométrie »). Les systèmes frustrés ont des propriétés nouvelles et remarquables. Ce qui est frappant est que des méthodes très puissantes telles que le groupe de renormalissation ont du mal à clarifier un certain nombre de points tels que la nature de la phase transition dans des systèmes de spins frustrés, comme on le verra dans cet article de revue. J'ai commencé à étudier des systèmes de spins frustrés au début des années 80, après ma thèse. J'ai bénéficié de nombreuses discussions avec Gérard Toulouse. Je continue mes recherches jusqu'aujourd'hui sur des systèmes frustrés tels que les skyrmions. Dans cette revue, j'évoque mes travaux représentatifs sur des systèmes frustrés, allant des systèmes frustrés de spins Ising exactement résolus aux systèmes de spins XY ou Heisenberg en 2D et 3D. J'évoquerai mes derniers travaux sur les skyrmions résultant de la compétition entre l'interaction d'échange et l'interaction Dzyaloshinskii–Moriya (DM) soumis à un champ magnétique appliqué. Enfin, une théorie

quantique de magnons utilisant la méthode de fonction de Green est présentée pour des systèmes frustrés avec des configurations de spin non-colinéaires tels que ceux avec l'interaction DM.

Keywords. Frustrated spin systems, Exactly solved models, Non-collinear spin configuration, Phase transitions, Reentrance, Disorder lines.

Mots-clés. Systèmes de spins frustrés, Modèles exactement solvables, Configurations de spin non-colinéaires, Skyrmions, Théorie de Magnons dans des Systèmes Frustrés.

Manuscript received 20 November 2024, revised 12 January 2025, accepted 17 January 2025.

1. Introduction

This paper is devoted to the memory of Gérard Toulouse. Since 1981, I was interested in the effects of frustation in spin systems, a few years after Toulouse [1] and Villain [2] independently introduced the notion of frustration. Note that in the early years of the 70's, the introduction of the renormalization group theory [3–6] and the exactly solved spin systems [7] have made a great progress in the understanding of the mechanism governing the phase transition: one can mention the distinction between first- and second-order phase transitions, the discovery of universality classes distinguished by critical exponents and the theory of finite-size scaling. Competing interactions have been studied in many investigations by these advanced methods but most of these studies are restrained to the cases where the spin ordering is collinear, namely ferromagnetic or antiferromagnetic (exceptions made for q-state Potts models [7]). The first frustrated spin system with non-collinear spin ordering is the helimagnetic structure discovered independently by Yoshimori [8] and Villain [9]: the competition between the ferromagnetic interaction between nearest neighbors (NN) $J_1 > 0$ and the antiferromagnetic interaction $J_2 < 0$ between next NN (NNN) results in a non-collinear spin configuration when $|J_2|/J_1$ is larger than a critical value. We return to this case below. The most popular case which has been widely studied since the 80's is the antiferromagnetic triangular lattice with vector spins (XY and Heisenberg spins). Note that the antiferromagnetic triangular lattice with Ising spins has been exactly solved in 1950 by Wannier [10, 11]. As will be recalled below, the ground state (GS) of the antiferromagnetic triangular lattice with vector spins is the well-known 120° structure. The nature of the phase transition in the case of stacked triangular lattices with vector spins has been subject of investigations for more than 30 years [12–19]. We will recall this case in this review. In the 80's I have studied alone or with collaborators a number of frustrated systems such as the fully frustrated simple cubic lattice [20–22] (Toulouse was a coauthor in [20]). Note that this system has been studied a few years before by Derrida et al. [23, 24]. I also studied during this period the helimagnets (spin waves and phase transition), the phase transition in the frustrated face-centered cubic (FCC) Heisenberg lattice and the frustrated Villain's model with XY spin model. Then I started with my colleagues a series of papers on exactly solved Ising frustrated models such as the generalized Kagomé lattices, honeycomb lattice and dilute centered square lattices. We found new striking phenomena such as multiple phase transitions, reentrance phases, disorder lines, and coexistence of order and disorder. I will show some of these results below. Going further into the frustration effects, I studied with colleagues the effect of Dzyaloshinskii–Moriya (DM) interaction in ferromagnetic and antiferromagnetic materials. As a result of the competition between collinear ordering and perpendicular spin ordering due to the DM interaction, non-collinear orderings are observed. Under a perpendicular applied magnetic field, the spin configuration can turn into skyrmions arranged on an ordered way which is called "skyrmion crystal". A skyrmion is a topologically stable vortex-like structure which contains a dozen of spins turning around a center. I will recall some of the results below.

Important works on many aspects of frustrated systems have been reviewed in a book [25]. The reader is referred to this reference for a rather complete bibliography.

This paper is a personal account of works on a subject inspired by the work of Toulouse on the frustration. In Section 2, I recall some elementary notions of the frustration and its effect on the GS. In Section 3, I review some results on exactly solved Ising frustrated systems. In Section 4, I present some results of my early works on frustrated systems either in collaboration with Toulouse or inspired by discussions with him. I also recall here results on the nature of the phase transition of other frustrated systems such as helimagnets, fully frustrated antiferromagnetic HCP and FCC lattices with vector spins. A brief account on the nature of the phase transition in the stacked antiferromagnetic triangular lattice is presented. Some basic results on skyrmions are discussed in Section 5. Finally, a quantum theory of magnons using the Green's function method for non-collinear spin configurations such as the ones in helimagnets and in systems with Dzyaloshinskii–Moriya is shown in Section 6. Concluding remarks are given in Section 7.

2. Frustration: introduction

Before introducing the definition of the frustration given by Toulouse [1] in the context of spin glasses, let us recall some early developments in the 60's and early 70's on spin glasses. The new quenching experimental method introduced by Pol Duwez [26] in 1960 has resulted in the fabrication on many metglasses (metallic glasses) in which bond disorder causes metastable states. The reader is referred to the reference [27] for reviews on works up to 1984 on metglasses. Several theoretical models of spin glasses have been published in the 70's. One can mention two of them: the Edwards–Anderson (EA) model [28] and the Sherrington–Kirpatrick (SK) model [29]. Spin glasses are viewed as systems having two main ingredients: bond disorder and frustration. In a spin glass, there is a random mixing of ferromagnetic and antiferromagnetic bonds between spins. This mixing causes the frustration as we will define below. The EA model consists of nearest-neighbor Ising spins interacting with each other via a pairwise random interaction. This model has been exactly solved by its authors using the replica method with the hypothesis that the random interactions obey a Gaussian distribution covering negative and positive values. The SK model was also based on the Ising spin model, however the spins interact with each other via an infinite range with a Gaussian distribution with positive and negative interactions. The SK model has also been solved by its authors using the replica method, but the entropy is found negative at low temperatures. This model was finally solved by a replica breaking ansatz introduced by Parisi in 1979 [30] where stable spin glass states at low T are found. The reader is referred to the book by Mézard, Parisi and Virasoro [31] for details on the replica method.

Let us note that in the early 80's numerical simulations have also been developped to study spin glasses. I myself started to write Monte Carlo programs to study several spin glass models. I mention here a few works I published with co-authors on spin glass using Monte Carlo simulations during this period [32–34]. In this period, there was the nice work of Ogielski [35] on the $\pm J$ Ising model on the simple cubic lattice, using Monte Carlo simulations. His results are in agreement with experiments performed on insulating spin glasses, despite the simplicity of the discrete model for spin glasses.

As said above, the two main ingredients of spin glass are bond disorder and frustration. The idea to separate the two ingredients to study systems with frustration but without bond disorder comes naturally: such frustrated systems having periodical $\pm$ bond distributions on the lattice are subject to exact treatment. This is what I have done in a series of papers on exactly solved models with my young team in the late 80's (see Section 3).

We have seen that the frustration is caused by the competition between various interactions in the system. However, the frustration can also be generated by only one type of interaction in the

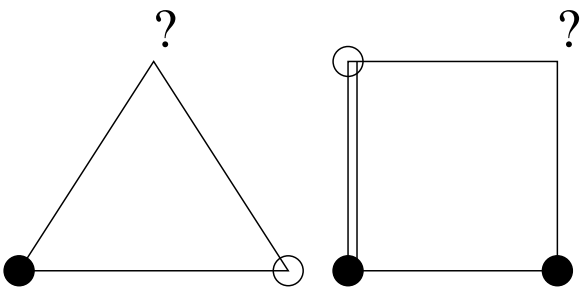

Figure 1. Examples of frustrated plaquettes: ferro- and antiferromagnetic interactions, J and $-J$, are shown by single and double lines, $\uparrow$ and $\downarrow$ Ising spins by black and void circles, respectively. Choosing any orientation for the spin marked by the question mark will leave one of its bonds unsatisfied (frustrated bond).

case where the lattice structure which does not allow to fully satisfy every interaction bond: this is the case of a triangular lattice with an antiferromagnetic interaction between nearest neighbors (NN), or the face-centered cubic (FCC) lattice and the hexagonal-closed-packed (HCP) lattice, with antiferromagnetic NN interaction. These latter cases are called "geometry frustration".

The effects of the frustration are numerous. We can mention a few of them (the reader is referred to chapter 1 of Ref. [25]): (i) the GS degeneracy is very high, in many cases the GS degeneracy is infinite, (ii) in the case of vector spins (XY and Heisenberg spins), the GS spin configuration is non-collinear, unlike the collinear configuration in ferromagnets and antiferromagnets. A famous example is the 120° spin structure in the antiferromagnetic triangular lattice (note that the helimagnetic structure has been determined a long time ago [8, 9] (iii) the nature of the phase transition is often difficult to determine. To our knowledge, the phase transition in most (if not all) frustrated systems in 3D is of the first-order transition. Well-known examples are the cases of HCP antiferromagnets [36, 37], the FCC antiferromagnets [38] and the antiferromagnetic stacked triangular lattice [12–19].

Let us examine some simple cases in the following.

2.1. *Definition*

We give below some popular cases for readers who are not familiar with frustrated spin systems.

In the pairwise Ising and Heisenberg model, the interaction energy between two spins $\mathbf{S}_i$ and $\mathbf{S}_j$ is given by $E = -J(\mathbf{S}_i \cdot \mathbf{S}_j)$ where $J > 0$ ($J < 0$) is the exchange integral giving rise to parallel (antiparallel) spin pairs. The minimum of E is $-J$ or $-|J|$. For a crystal where the NN interaction is ferromagnetic, the GS of the system corresponds to the spin configuration where all spins are parallel. This is true for any lattice structure. However, if J is antiferromagnetic, the spin configuration of the GS depends on the lattice structure: (i) for lattices containing no elementary triangles, such as square lattice and simple cubic lattices, the GS is the configuration in which each spin is antiparallel to its neighbors, namely every bond is fully satisfied (lowest energy); (ii) for lattices containing elementary triangles such as the triangular lattice, the FCC and HCP lattices, it is impossible to construct a GS where all bonds have the lowest energy J (see Figure 1): The GS does not correspond to the minimum of the interaction of every spin pair. In this case, one says that the system is frustrated.

Let us recall the frustration defined by Toulouse: one considers an elementary cell of the lattice. The lattice cell is in general a polygon formed by faces hereafter called "plaquettes". For example, the elementary cell of the simple cubic (SC) lattice is a cube with six square plaquettes, the elementary cell of the FCC lattice is a tetrahedron formed by four triangular plaquettes. Let

$J_{i,j}$ be the interaction between two NN spins of the plaquette. According to the definition of Toulouse [1], the plaquette is frustrated if the parameter P defined below is negative

$$P = \prod_{\langle i,j \rangle} \text{sign}(J_{i,j}), \tag{1}$$

where the product is performed over all $J_{i,j}$ around the plaquette. Two examples of frustrated plaquettes are shown in Figure 1: a triangle with three antiferromagnetic bonds and a square with three ferromagnetic bonds and one antiferromagnetic bond. P is negative in both cases. One sees that if one tries to put Ising spins on those plaquettes, at least one of the bonds around the plaquette will not be satisfied. For vector spins, we show below that in the lowest energy state, each bond is only partially satisfied.

We consider another spin system, which can be called frustrated system because each bond is only partially satisfied: this is the case with different kinds of conflicting interactions and the GS does not correspond to the minimum of each kind of interaction. Let us examine a chain of spins where the NN interaction J_1 is ferromagnetic while the next NN (NNN) interaction J_2 is antiferromagnetic. As long as $|J_2| \ll J_1$, the GS is ferromagnetic: every NN bond is then satisfied but the NNN ones are not. Of course, when $|J_2|$ exceeds a critical value, the ferromagnetic GS is no longer valid (see the helimagnet example below): both the NN and NNN bonds are not fully satisfied.

Let us touch upon the GS degeneracy. One notes that for the triangular plaquette, the degeneracy is three, and for the square plaquette it is four, in addition to the degeneracy associated with global spin reversal. Therefore, the degeneracy of an infinite lattice composed of such plaquettes is infinite, in contrast to the unfrustrated case.

At this stage, it is worth noting that in the above discussion we have assumed the interaction between two spins to be of the form $E = -J(\mathbf{S}_i \cdot \mathbf{S}_j)$. However, the frustration takes place also in systems with other types of interaction such as the Dzyaloshinski–Moriya interaction $E = -\mathbf{D} \cdot (\mathbf{S}_i \wedge \mathbf{S}_j)$: a spin system is frustrated whenever the minimum of the system energy does not correspond to the minimum of all local interactions, whatever the form of interaction. In such a case, the definition of frustration is more general than the one using Equation (1).

The determination of the GS of various frustrated Ising spin systems such as the Kagomé lattice, the honeycomb lattice and the Union-Jack lattice, as well as discussions on their thermodynamic properties using exactly solved methods have been presented in Ref. [39]. In the following section, we recall the GS of a few frustrated systems with XY and Heisenberg spins.

2.2. *Non-collinear spin configurations*

Consider again the plaquettes shown in Figure 1. In the case of XY spins, one can calculate the GS configuration by minimizing the energy of the plaquette E while keeping the spin modulus constant. In the case of the triangular plaquette, suppose that spin $\mathbf{S}_i$ ($i = 1,2,3$) of amplitude S makes an angle θ_i with the Ox axis. Writing E and minimizing it with respect to the angles θ_i, one has

$$\begin{aligned}
E &= J(\mathbf{S}_1 \cdot \mathbf{S}_2 + \mathbf{S}_2 \cdot \mathbf{S}_3 + \mathbf{S}_3 \cdot \mathbf{S}_1) \\
&= JS^2 \left[\cos(\theta_1 - \theta_2) + \cos(\theta_2 - \theta_3) + \cos(\theta_3 - \theta_1)\right], \\
\frac{\partial E}{\partial \theta_1} &= -JS^2 \left[\sin(\theta_1 - \theta_2) - \sin(\theta_3 - \theta_1)\right] = 0, \\
\frac{\partial E}{\partial \theta_2} &= -JS^2 \left[\sin(\theta_2 - \theta_3) - \sin(\theta_1 - \theta_2)\right] = 0, \\
\frac{\partial E}{\partial \theta_3} &= -JS^2 \left[\sin(\theta_3 - \theta_1) - \sin(\theta_2 - \theta_3)\right] = 0.
\end{aligned}$$

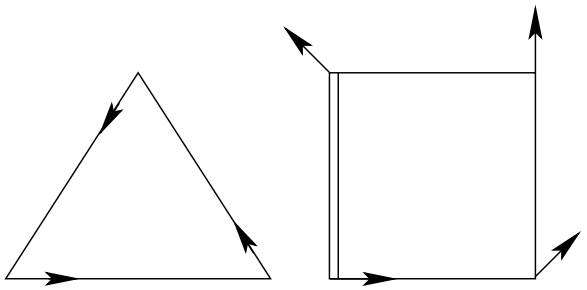

Figure 2. Non-collinear spin configuration of frustrated triangular and square plaquettes with XY spins: ferro- and antiferromagnetic interactions J and $-J$ are indicated by thin and double lines, respectively.

A solution of the last three equations is $\theta_1-\theta_2=\theta_2-\theta_3=\theta_3-\theta_1=2\pi/3$. This solution can be also obtained by writing the following equality

$$E=J(\mathbf{S}_1\cdot\mathbf{S}_2+\mathbf{S}_2\cdot\mathbf{S}_3+\mathbf{S}_3\cdot\mathbf{S}_1)=-\frac{3}{2}JS^2+\frac{J}{2}(\mathbf{S}_1+\mathbf{S}_2+\mathbf{S}_3)^2.$$

The minimum of the above equation evidently corresponds to $\mathbf{S}_1+\mathbf{S}_2+\mathbf{S}_3=0$ which yields, using a geometric construction, the 120° structure. This is true also for Heisenberg spins.

We can do the same calculation for the case of the frustrated square plaquette [40]. Suppose that the antiferromagnetic bond $-\eta J$ connects the spins $\mathbf{S}_1$ and $\mathbf{S}_2$ and the ferromagnetic bond is J ($J>0$). We find

$$\theta_2-\theta_1=\theta_3-\theta_2=\theta_4-\theta_3=\frac{\pi}{4}\quad\text{and}\quad\theta_4-\theta_1=\frac{3\pi}{4}. \tag{2}$$

If the antiferromagnetic bond is equal to $-\eta J$, the solution for the angles is [40]

$$\cos\theta_{32}=\cos\theta_{43}=\cos\theta_{14}\equiv\cos\theta=\frac{1}{2}\left[\frac{\eta+1}{\eta}\right]^{1/2} \tag{3}$$

and $|\theta_{21}|=3|\theta|$, where $\cos\theta_{ij}\equiv\cos(\theta_i-\theta_j)$.

This solution exists if $|\cos\theta|\le 1$, namely $\eta>\eta_c=1/3$. One can check that when $\eta=1$, one has $\theta=\pi/4$, $\theta_{21}=3\pi/4$.

We show the frustrated triangular and square lattices in Figure 2 with XY spins ($N=2$).

One observes that there is a two-fold degeneracy resulting from the symmetry by mirror reflecting with respect to an axis, for example the y axis in Figure 2. Therefore the symmetry of these plaquettes is of Ising type O(1), in addition to the symmetry SO(2) due to the invariance by global rotation of the spins in the plane.

Another example is the case of a chain of Heisenberg spins with ferromagnetic interaction $J_1(>0)$ between NN and antiferromagnetic interaction $J_2(<0)$ between NNN. When $\varepsilon=|J_2|/J_1$ is larger than a critical value ε_c, the spin configuration of the GS becomes non-collinear. One shows that the helical configuration displayed in Figure 3 is obtained by minimizing the interaction energy (see [41–43]):

$$\begin{aligned}
E &= -J_1\sum_i\mathbf{S}_i\cdot\mathbf{S}_{i+1}+|J_2|\sum_i\mathbf{S}_i\cdot\mathbf{S}_{i+2}\\
&= S^2\,[-J_1\cos\theta+|J_2|\cos(2\theta)]\sum_i 1\\
\frac{\partial E}{\partial\theta} &= S^2\,[J_1\sin\theta-2|J_2|\sin(2\theta)]\sum_i 1=0\\
&= S^2\,[J_1\sin\theta-4|J_2|\sin\theta\cos\theta]\sum_i 1=0,
\end{aligned} \tag{4}$$

where one has supposed that the angle between NN spins is θ.

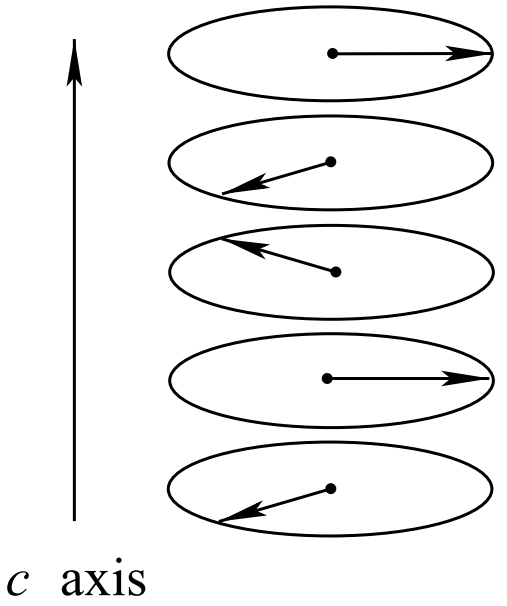

Figure 3. Helical configuration when $\varepsilon = |J_2|/J_1 > \varepsilon_c = 1/4$ ($J_1 > 0$, $J_2 < 0$).

The two solutions are

$$\sin\theta = 0 \longrightarrow \theta = 0 \quad \text{(ferromagnetic solution)}$$

and

$$\cos\theta = \frac{J_1}{4|J_2|} \longrightarrow \theta = \pm \arccos\left(\frac{J_1}{4|J_2|}\right). \tag{5}$$

The last solution is possible if $-1 \le \cos\theta \le 1$, i.e. $J_1/(4|J_2|) \le 1$ or $|J_2|/J_1 \ge 1/4 \equiv \varepsilon_c$.

As before, there are two degenerate configurations: clockwise and counter-clockwise.

We generate a triangular lattice using plaquettes as shown in Figure 4. The GS corresponds to the state where all triangle plaquettes of the same orientation have the same chirality: plaquettes $\triangle$ have positive chirality and plaquettes $\triangledown$ have negative chirality. Mapping the chiralities into the Ising spins, we have a perfect antiferromagnetic Ising order. This order is broken at a phase transition temperature where the chirality vanishes.

3. Exactly solved frustrated models

As seen in the following, frustrated systems are very difficult to deal with because of the GS degeneracy and the GS symmetry. They are excellent candidates to test approximations and improve theories. Since it is hard to relate observed phenomena to real mechanisms in real systems (disordered systems, systems with long-range interaction, three-dimensional systems, etc), it is worth to search for the origins of those phenomena in exactly solved systems. These exact results will help to understand at least qualitatively the behavior of real systems which are in general much more complicated.

We have exactly solved a number of 2D frustrated Ising model going from the Kagomé model with NNN interaction to an anisotropic frustrated honeycomb lattice, in passing by various frustrated models [44–48]. The reader is referred to [39] or to the original papers for a full description of the methods and results. Hereafter, we underline only the conditions for finding exact solutions, and enumerate the most striking features we found.

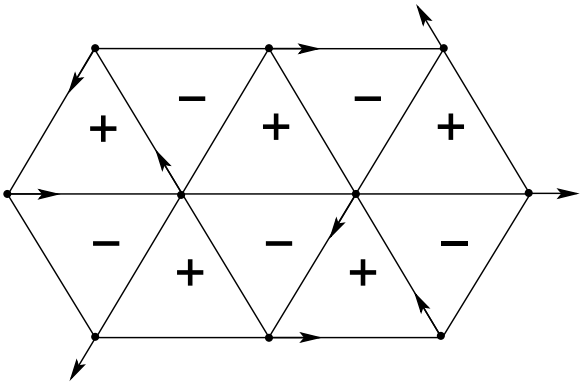

Figure 4. Antiferromagnetic triangular lattice with XY spins. The positive and negative chiralities are indicated by + and −.

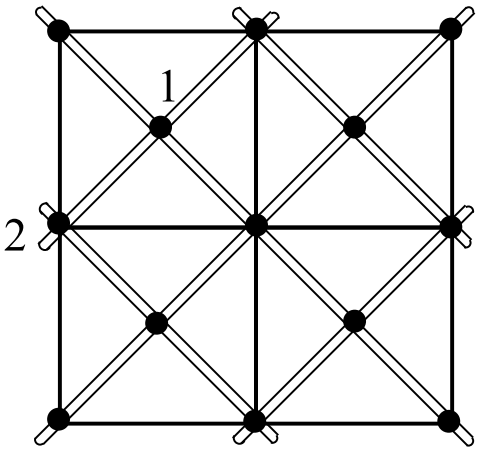

Figure 5. Centered square lattice. Interactions between NN and NNN, J_1 and J_2, are denoted by double and single bonds, respectively. The two sublattices are numbered 1 and 2.

Let us note that different 2D Ising models without crossing interactions can be mapped onto the 16-vertex model or the 32-vertex model, with the free-fermion condition automatically satisfied in such cases. The partition function can be exactly found, leading to the critical condition allowing to determine the phase transition as a function of interaction parameters.

The frustrated 2D Ising centered square lattice has been exactly solved by Vaks et al. [49] even before the notion of frustration was introduced [1] (see Figure 5 with NN and NNN interactions, J_1 and J_2, respectively). The ground state properties of this model are as follows: for $a = J_2/|J_1| > -1$, spins of sublattice 2 orders ferromagnetically and the spins of sublattice 1 are parallel (antiparallel) to the spins of sublattice 2 if $J_1 > 0$ (<0); for $a < -1$, spins of sublattice 2 orders antiferromagnetically, leaving the centered spins free to flip.

The phase diagram of this model in the space $(a = J_2/|J_1|, T)$ is shown in Figure 6.

It is interesting to note that (i) in a small interval above $a = 1$, when one increases T, the system goes from the ferromagnetic (F) phase to the narrow paramagnetic phase between F and AF phases, then enters the partially ordered phase AF before going to the high-T paramagnetic phase. In the AF phase the centered spins are free to flip as said above. The narrow paramagnetic

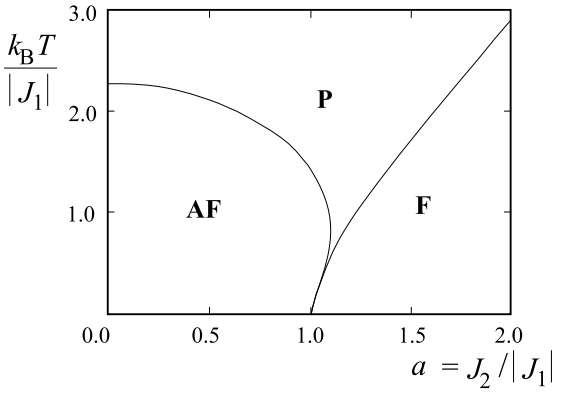

Figure 6. Phase diagram of centered square lattice [49]. See text for comments.

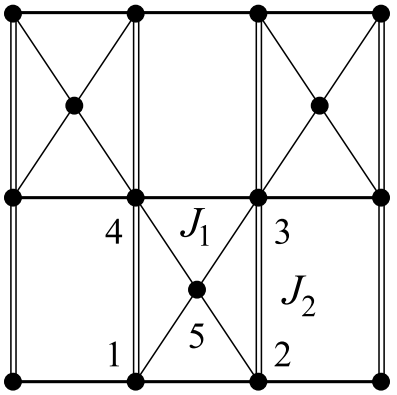

Figure 7. Kagomé lattice. Interactions between NN and between NNN, J_1 and J_2, are shown by single and double bonds, respectively. The lattice sites in a cell are numbered for decimation demonstration (not shown).

phase between F and AF phases is called "reentrance phase" (a disordered phase between two ordered phases).

Let us consider as another example of the Ising model defined on a Kagomé lattice, with two-spin interactions NN and NNN, J_1 and J_2, respectively, as shown in Figure 7.

The Hamiltonian is written as

$$H = -J_1 \sum_{(ij)} \sigma_i \sigma_j - J_2 \sum_{(ij)} \sigma_i \sigma_j \tag{6}$$

where and the first and second sums run over the spin pairs connected by single and double bonds, respectively. Note that the model without J_2 has been exactly solved a long time ago [50] showing no phase transition at finite T when J_1 is antiferromagnetic. Taking into account the NNN interaction J_2 (see Figure 7 and Equation (6)), we have solved [44] this model by transforming it into a 16-vertex model which satisfies the free-fermion condition. Let us just show the phase diagram in the space $(J_2/J_1, T)$ in Figure 8. There are three remarkable points: (i) the X phase is a partially disordered phase (only centered spins are disordered), (ii) the reentrance phase (paramagnetic phase between X and F phases near the endpoint, (iii) the existence of a disorder line starting from the endpoint, separating the paramagnetic phase of F from that of X (see signification of the disorder line in [51–53]). These points are very interesting, they

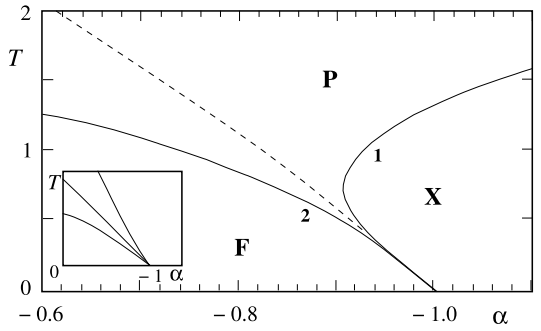

Figure 8. Phase diagram of the Kagomé lattice with NN and NNN interactions in the region $J_1 > 0$ of the space $(\alpha = J_2/J_1, T)$. T is measured in the unit of J_1/k_B. Solid lines are critical lines, dashed line is the disorder line. P, F and X stand for paramagnetic, ferromagnetic and partially disordered phases, respectively. The inset shows schematically enlarged region of the endpoint.

exist in highly frustrated solvable models but we believe that some real systems may bear some similar aspects. In the other models that we have studied [45–47], these properties are even more striking. The reader is referred to [39] for more discussion.

It is interesting to note that the reentrance phase and the partial disorder found in the exactly solved models shown above exist also in quantum frustrated systems in three dimensions [54–56] using Green's function and Monte Carlo methods.

4. Fully frustrated systems and some other frustrated systems

Several works in collaboration with Toulouse have been carried out on the so-called "fully frustrated simple cubic (SC) lattice" which is made by stacking the cubic cell shown in Figure 9 [20–24]. Let us say a few words on the work in which Toulouse was involved. Classical vector spins on the sites of this lattice interacting via a periodic fully frustrated array of exchange interactions exhibit an interesting manifold of GS configurations. In particular, for Heisenberg spins, the manifold has dimension 5, with two continuous degeneracy parameters, in addition to global rotation angles. A configuration space analysis, including pair and triangle overlap statistics, has been performed for this test model. The reader is referred to the original paper [20] for details of the calculations. We also studied the phase transition of this lattice with Ising [21], XY and Heisenberg spins [22]. Note that in the XY case, using an algorithm which minimizes the local energies, we find twelve periodic GS spin configurations. A 12-fold degeneracy is very rare, if not unique, for a XY spin system. In the case of Heisenberg spins, the degeneracy is infinite. The phase transion in the case has been clarified after 30 years of uncertainty: using the high-performance Wang–Landau flat histogram MC algorithm [57–61] we have shown that the transition is of first order for both XY and Heisenberg spins [62, 63]: the energy histogram shown in Figure 10 has a double-peak structure at the transition temperature which is a signature of a first-order transition: the distance between the two peaks is the latent heat.

Let us summarize some frustrated systems having a first-order transition:

- Helimagnets with vector spins have a first-order transition [36, 37].
- Antiferromagnetic FCC lattice with Heisenberg spin has a first-order transition [38].
- $J_1 - J_2$ SC model with Heisenberg spins [64], with Ising spins [65] both have first-order transition.

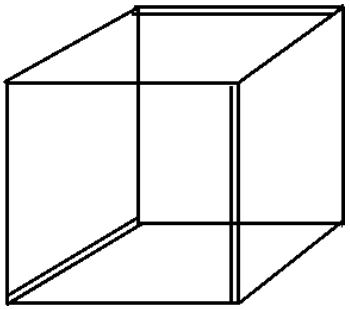

Figure 9. Unit cell of a fully SC lattice. Double (simple) line is antiferromagnetic (ferromagnetic) interaction. Note that every face of the cell is frustrated. The full lattice is made by stacking this cell in all space directions. It is called fully frustrated SC lattice.

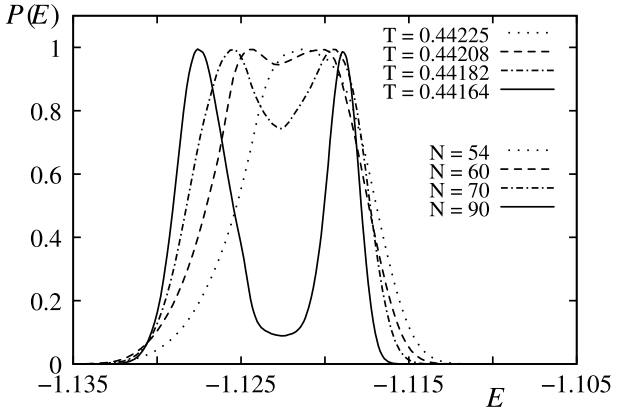

Figure 10. Fully frustrated SC lattice with Heisenberg spins: Energy histogram for several sizes $N = 54, 60, 70, 90$ at T_c indicated on the figure. See text for comments.

- The stacked triangular antiferromagnets: this model has been a fascinating subject since the 80's [12, 13]. Different methods give different results on the order of the phase transition. The very recent papers [16, 17] confirm the first-order nature found by non-perturbative renormalization group [14, 15] and by Wang–Landau method [18, 19]. The reader is referred to the papers [16, 17] for a complete bibliography on this subject.

To conclude this section, let us emphasize that the so-called zigzag model in 2D with XY spin model (Figure 11) shows a remarkable property: as the symmetry of the GS is two-fold (positive and negative chiralities), the breaking of this symmetry is of Ising type. However, the XY nature of the spins affects the criticality: we have shown in Ref. [66] that (i) the Ising and XY symmetries are broken at the same temperature (a single transition) (ii) the values of the critical exponents are $\nu = 0.852(2)$ and $\gamma = 1.531(3)$, better than most earlier MC results, in agreement with the suggestion of a coupled "XY Ising" universality class by Lee et al. [67–70]. This is a new kind of criticality.

5. Skyrmions

Skyrmions are topologically stable spin structures observed in various materials and theories. They are objects of intensive studies since 2003 after the work of A. Bogdanov [71]. We just cite

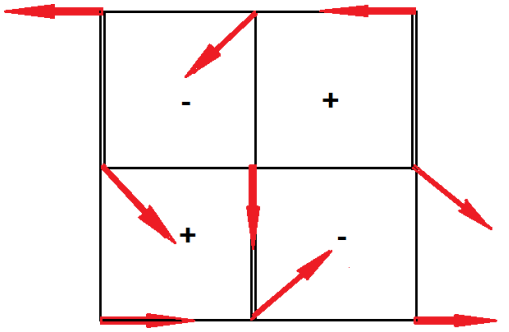

Figure 11. The XY zigzag model: double and single lines are antiferromagnetic ($J = -1$) and ferromagnetic ($J = 1$), respectively. The angle between two neighboring spins linked by a ferromagnetic bond is 45° and that between spins linked by an antiferromagnetic bond is 135° (see the paragraph below Equation (3)). The chiralities "+" and "−" are noted on the plaquettes of the spin configuration. See text for comments.

a few works hereafter. The rapid development of the field of skyrmions is due to the potential applications using skyrmions in spintronics [72–78].

Skyrmions are generated by various interaction mechanisms. They can result from over-frustrated spin systems under an applied magnetic field [79, 80] or from the Dzyaloshinskii–Moriya interaction (DMI) as seen in [81–84] among many other works in the literature. Note that a single skyrmion consists of a spin pointing down at the center. The surrounding spins turn around the center with incrreasing z component when going away the center. At the boundary, all spins are up. There are two kinds of such arrangement. The first kind is the Bloch-type skyrmion in which the spins rotate in the tangential planes, namely perpendicular to the radial directions, when moving from the core to the periphery. The second kind is the Neel-type skyrmion in which the spins rotate in the radial planes from the core to the periphery [85]. In our model shown below, only the Bloch-type skyrmions are observed.

Hereafter, I take a recent work to illustrate some basic properties of a system with a DMI [84]. Consider an antiferromagnetic triangular lattice with the following Hamiltonian

$$\mathscr{H} = -J\sum_{\langle ij\rangle} \mathbf{S_i}\cdot\mathbf{S_j} - D\sum_{\langle ij\rangle} \mathbf{u}_{i,j}\cdot\mathbf{S_i}\times\mathbf{S}_j - H\sum_i S_i^z \tag{7}$$

where $\mathbf{S_i}$ is a classical Heisenberg spin of magnitude 1 occupying the lattice site i. The first sum runs over all spin nearest-neighbor (NN) pairs with an antiferromagnetic exchange interaction J ($J < 0$), while the second sum is performed over all DM interactions between NN. H is the magnitude of a magnetic field applied along the z direction perpendicular to the lattice xy plane. The D-vector of the DMI is taken perpendicular to the xy plane and is given by

$$\mathbf{D}_{i,j} = D\mathbf{u}_{i,j} \tag{8}$$

$$\mathbf{D}_{j,i} = D\mathbf{u}_{j,i} = -D\mathbf{u}_{i,j} \tag{9}$$

where $\mathbf{u}_{i,j}$ is the unit vector on the z axis, and D represents the DM interaction strength.

The calculations of the GS have been done in details in [84] for the case of perpendicular **D** where ($D \neq 0$, $J = 0$, $H = 0$), ($D \neq 0$, $J \neq 0$, $H = 0$), and ($D \neq 0$, $J \neq 0$, $H \neq 0$). The first two cases have been done by analytically minimizing the Hamiltonian and the last case by the numerical steepest descent method. The results of the first two cases are shown in Figure 12.

Now, we take the case of in-plane $\mathbf{D}_{i,j}$: we define $\mathbf{D}_{i,j}$ as

$$\mathbf{D}_{i,j} = D(\mathbf{r}_j - \mathbf{r}_i)/|\mathbf{r}_j - \mathbf{r}_i| = D\mathbf{r}_{ij} \tag{10}$$

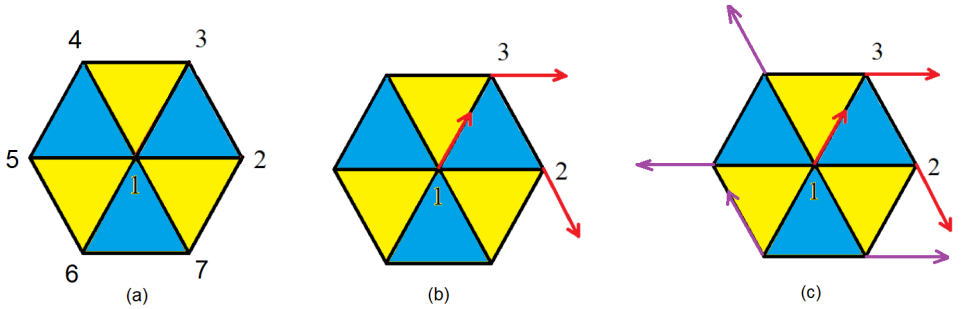

Figure 12. Perpendicular $\mathbf{D}_{i,j}$: (a) The spins on a hexagon are numbered as indicated; (b) Ground-state spin configuration with only Dzyaloshinskii–Moriya interaction on the triangular lattice ($J = 0$) is analytically determined. One angle is 120°, the other two are 60°. Note that the choice of the 120° angle in this figure is along the horizontal spin pair. This configuration is one ground state, the other two ground states have the 120° angles on respectively the two diagonal spin pairs. Note also that the spin configuration is invariant under the global spin rotation in the xy plane; (c) example of construction of the GS for the whole hexagon: spins in violet are added in respecting the turning angle in each direction. See calcullations in Ref. [84].

where D is a constant and $\mathbf{r}_{ij}$ denotes the unit vector along $\mathbf{r}_j - \mathbf{r}_i$. The GS in this case is determined by the numerical steepest descent method. With ($D \neq 0$, $J \neq 0$) under an applied field H, the result is shown in Figure 13 for $J = -1$, $D = 0.5$ and $H = 3$. One observes the three interpenetrating skyrmion sublattices.

These results are in agreement with early works using laborious MC simulations at low T [86–89].

To see if the skyrmions are stable at finite T, we have performed MC simulations. In addition to the internal energy E and the specific heat C_v, we calculated the order parameter Q defined as the projection of the spin confuguration at the time t at a given temperature T on the GS. These quantities are given by

$$\langle E\rangle = \langle \mathscr{H}\rangle/(2N) \tag{11}$$

$$C_v = \frac{\langle E^2\rangle - \langle E\rangle^2}{k_{\rm B}T^2} \tag{12}$$

$$Q(T) = \frac{1}{N(t_a - t_0)}\sum_i \left|\sum_{t=t_0}^{t_a} \mathbf{S}_i(T,t)\cdot\mathbf{S}_i(T=0)\right| \tag{13}$$

where $t_a - t_0$ is the averaging time. Note that the order parameter Q mimics the Edwards–Anderson order parameter [28] defined for random spin configurations (spin glass). The results are shown in Figure 14 where the z component M_z is also displayed. We observe a transition from the skyrmion phase to the paramagnetic phase at $T_{\rm c}/|J| \simeq 0.35$ where C_v shows a peak, and where Q vanishes (the non zero values of Q and M_z after $T_{\rm c}$ are due to the applied field). The stability of skyrmions at finite temperatures is essential because devices based on skyrmions are helpful only if they work at finite T.

Note that the size of the skyrmion does not depend on the lattice size when it is larger than 40×40 (smaller sizes induce some boundary effects). The skyrmion size depends however on the strength of the applied field H: the stronger H, the smaller the diameter of the skyrmion. The results shown in Figure 14 were obtained with the size 100×100. The size effects for larger sizes are insignificant. As the last remark, we do not know at the time being about the nature of the

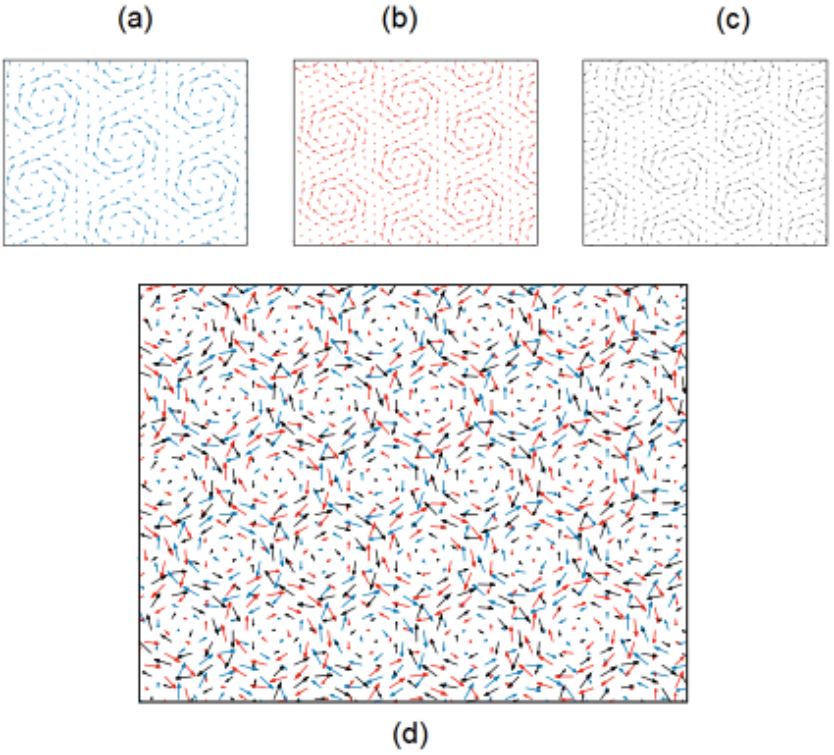

Figure 13. In-plane $\mathbf{D}_{i,j}$: the skyrmion crystal observed at $J = -1$, $D = 0.5$ and $H = 3$: a portion of skyrmion sublattice 1, 2 and 3 is respectively shown in (a), (b) and (c). Figure (d) shows the three interpenetrating antiferromagnetic skyrmion sublattices distinguished by three colors.

transition observed here. A question which naturally arises is that whether or not it follows the standard finite-size scaling theory of a second-order phase transition (see [5, 6] for a summary of this theory). It needs a further study to clarifdy this point.

To conclude this section, we note that what shown above is some basic properties of skyrmions. The dynamics of skyrmions which is the heart of applications in spintronics, is not presented here to keep a reasonable length of the paper. We note however that the small size of skyrmions (a dozen of spins), their topologically protected stability and their easy mobility [75, 77, 85] make them very suitable for applications. The reader is referred to more references cited in this paper on this subject, from Ref. [71] to Ref. [89] (the titles tell much about their contents).

6. Quantum theory for non-collinear spin configurations: Green's function method

The study of elementary excitations in spin systems is one of the main subjects in magnetism [90]. In magnetic materials, elementary excitations, called "spin waves" or "magnons", dominate the low-temperature properties. Various means of investigation, theoretically and experimentally, such as spin-wave theories and inelastic neutron scattering, have been developped since the 60's for magnetic materials. Theoretically, the theory of magnons based on the Holstein-Primakoff was the most advanced theory, but the validity of this method is limited to the region of very low temperatures [90]. The first Green's function method introduced by Zubarev in 1960 [91] allowed us to calculate bulk magnetic properties up to the transition temperature T_C. I have applied

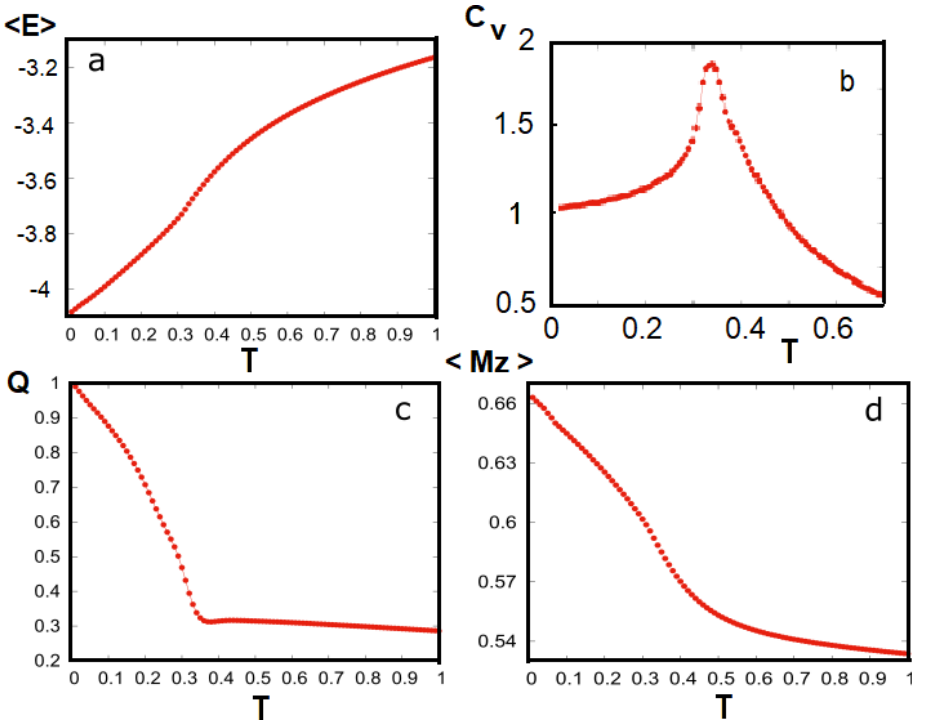

Figure 14. Results for $J = -1$, $D = 0.5$, $H = 3$: (a) Energy vs T, (b) Specific heat vs T, (c) Order parameter vs T, (d) z-component of the magnetization versus T.

this method with success in a study of magnetic thin films in 1979 [92]. Note that these studies have been limited to the cases where the magnetic ordering is collinear. I have developped with R. Quartu a Green's function technique in 1997 to study non-colinear spin configurations [54] in frustrated spin systems: we observe that the commmutation relations between spin-deviation operators are valid only when the spin lies on its quantization axis. However, in a non-collinear configuration, each spin has its own quantization axis. Our idea was, for a given spin, to use its "local coordinates". The calculation was possible for any non-collinear spin configuration, as seen in our publications afterward: one can mention the case of frustrated surface in thin films [93, 94] or helimagnetic thin films [95] where the surface spin reconstruction is strong. Surface effects in thin films have been widely studied theoretically, experimentally, and numerically, during the last three decades [96, 97]. Nevertheless, surface effects in frustrated systems such as helimagnets have only been recently studied: surface spin structures [98], MC simulations [99], magnetic field effects on the phase diagram in Ho [100], and a few experiments [101, 102]. Helical magnets present potential applications in spintronics with predictions of spin-dependent electron transport in these magnetic materials [103–105]. In the following, I recall the main steps of the calculation, the reader is referred to the original paper [95] for more details.

6.1. *Green's function method for helimagnets*

To illustrate the method, let us consider the simplest case of helimagnets: the turn angle takes place in the c-direction of a body-centered tetragonal (BCT) lattice, perpendicular to the film. This is due to the NNN antiferromagnetic interaction $J_2 < 0$ in that direction. For NN interaction,

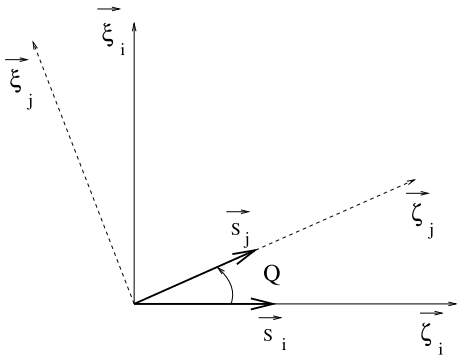

Figure 15. Local coordinates in a xy-plane perpendicular to the c-axis. Q denotes $\theta_j - \theta_i$.

Table 1. Values of $\cos\theta_{n,n+1} = \alpha_n$ between two adjacent layers are shown for various values of J_2/J_1

J_2/J_1	$\cos\theta_{1,2}$	$\cos\theta_{2,3}$	$\cos\theta_{3,4}$	$\cos\theta_{4,5}$	α(bulk)
−1.2	0.985(9.79°)	0.908(24.73°)	0.855(31.15°)	0.843(32.54°)	33.56°
−1.4	0.955(17.07°)	0.767(39.92°)	0.716(44.28°)	0.714(44.41°)	44.42°
−1.6	0.924(22.52°)	0.633(50.73°)	0.624(51.38°)	0.625(51.30°)	51.32°
−1.8	0.894(26.66°)	0.514(59.04°)	0.564(55.66°)	0.552(56.48°)	56.25°
−2.0	0.867(29.84°)	0.411(65.76°)	0.525(58.31°)	0.487(60.85°)	60°

Only angles of the first half of the 8-layer film are shown: other angles are, by symmetry, $\cos\theta_{7,8} = \cos\theta_{1,2}$, $\cos\theta_{6,7} = \cos\theta_{2,3}$, $\cos\theta_{5,6} = \cos\theta_{3,4}$. The values in parentheses are angles in degrees. The last column shows the value of the angle in the bulk case (infinite thickness). For presentation, angles are shown with two digits.

we assume a ferromagnetic interaction $J_1 > 0$. The film thickness consists of N_z layer. In the xy plane, we use the periodic boundary conditions. The hamiltonian is given by

$$\mathscr{H}_e = -\sum_{\langle i,j\rangle} J_1 \mathbf{S}_i \cdot \mathbf{S}_j - \sum_{\langle i,j\rangle} J_2 \mathbf{S}_i \cdot \mathbf{S}_j \tag{14}$$

where $\mathbf{S}_i$ and $\mathbf{S}_j$ are two quantum Heisenberg spins occupying the lattice sites i and j. The first and second sums run over the NN and NNN spin pairs, respectively.

For the bulk BCT lattice, modifying the method to obtain Equation (5) for a chain, we obtain the critical value $|J_2|/J_1 > 1$ above which the GS is helical.

Now, in a film there is a lack of NN and NNN at the two surfaces. This modifies the turn angle at and near the surfaces. The reader is referreed to Ref. [95] for the calculations. The results are shown in Table 1.

In the following, using the spin configuration obtained at each J_2/J_1 we calculate the spin-wave excitation and properties of the film such as the zero-point quantum spin fluctuations, the layer magnetizations versus T and the critical temperature T_C.

As said earlier, we have to use the local coordinates where a given spin should lie on its quantization axis. Needless to say, in a non-collinear spin configfuration, each spin has its own quantization axis. Let us show for a spin pair ($\mathbf{S}_i$, $\mathbf{S}_j$) the local coordinates shown in Figure 15: the quantization axis of spin $\vec{S}_i$ is on its ζ_i axis which lies in the plane, the η_i axis of $\vec{S}_i$ is along the c-axis, and the ξ_i axis forms with η_i and ζ_i axes a direct trihedron.

Since the spin configuration is planar, all spins have the same η axis. Furthermore, all spins in a given layer are parallel. Let $\hat{\xi}_i$, $\hat{\eta}_i$ and $\hat{\zeta}_i$ be the unit vectors on the local (ξ_i, η_i, ζ_i) axes. We write

$$\vec{S}_i = S_i^x \hat{\xi}_i + S_i^y \hat{\eta}_i + S_i^z \hat{\zeta}_i \tag{15}$$

$$\vec{S}_j = S_j^x \hat{\xi}_j + S_j^y \hat{\eta}_j + S_j^z \hat{\zeta}_j \tag{16}$$

We have (see Figure 15)

$$\begin{aligned}
\hat{\xi}_j &= \cos\theta_{ij}\hat{\zeta}_i + \sin\theta_{ij}\hat{\xi}_i \\
\hat{\zeta}_j &= -\sin\theta_{ij}\hat{\zeta}_i + \cos\theta_{ij}\hat{\xi}_i \\
\hat{\eta}_j &= \hat{\eta}_i
\end{aligned}$$

where $\cos\theta_{ij} = \cos(\theta_i - \theta_j)$ is the angle between two spins i and j. Replacing these into Equation (16) to express $\vec{S}_j$ in the $(\hat{\xi}_i, \hat{\eta}_i, \hat{\zeta}_i)$ coordinates, then calculating $\vec{S}_i \cdot \vec{S}_j$, we obtain the following exchange Hamiltonian from (14):

$$\begin{aligned}
\mathscr{H}_e = -\sum_{\langle i,j\rangle} J_{i,j} \Big\{ &\frac{1}{4}(\cos\theta_{ij} - 1)(S_i^+ S_j^+ + S_i^- S_j^-) + \frac{1}{4}(\cos\theta_{ij} + 1)(S_i^+ S_j^- + S_i^- S_j^+) \\
&+ \frac{1}{2}\sin\theta_{ij}(S_i^+ + S_i^-)S_j^z - \frac{1}{2}\sin\theta_{ij} S_i^z (S_j^+ + S_j^-) + \cos\theta_{ij} S_i^z S_j^z \Big\}
\end{aligned} \tag{17}$$

where the sum is performed on both NN and NNN spin pairs with corresponding exchange interactions J_{ij} and corresponding angles θ_{ij}.

Let us note that according to the theorem of Mermin and Wagner [106] continuous isotropic spin models such as XY and Heisenberg spins do not have long-range ordering at finite temperatures in two dimensions. The Heisenberg model in a thin film, of small thickness, though not in 2D, may need a small anisotropic interaction to enhance its long-range ordering at finite temperatures. We add therefore the following anisotropic interaction along the in-plane local spin-quantization axes z of $\mathbf{S}_i$ and $\mathbf{S}_j$:

$$\mathscr{H}_a = -\sum_{\langle i,j\rangle} I_{i,j} S_i^z S_j^z \cos\theta_{ij} \tag{18}$$

where $I_{i,j} (> 0)$ is supposed to be positive, very small compared to J_1, and limited to NN on the c-axis. The full Hamiltonian is thus $\mathscr{H} = \mathscr{H}_e + \mathscr{H}_a$.

We define the following two double-time Green's functions in the real space:

$$G_{i,j}(t,t') = \langle\langle S_i^+(t); S_j^-(t')\rangle\rangle = -\mathrm{i}\theta(t-t')\langle[S_i^+(t), S_j^-(t')]\rangle \tag{19}$$

$$F_{i,j}(t,t') = \langle\langle S_i^-(t); S_j^-(t')\rangle\rangle = -\mathrm{i}\theta(t-t')\langle[S_i^-(t), S_j^-(t')]\rangle \tag{20}$$

We need these two functions because the equation of motion of the first function generates functions of the second type, and vice-versa. These equations of motion are

$$\mathrm{i}\hbar\frac{\mathrm{d}}{\mathrm{d}t}G_{i,j}(t,t') = \langle[S_i^+(t), S_j^-(t')]\rangle\delta(t-t') - \langle\langle[\mathscr{H}, S_i^+(t)]; S_j^-(t')\rangle\rangle, \tag{21}$$

$$\mathrm{i}\hbar\frac{\mathrm{d}}{\mathrm{d}t}F_{i,j}(t,t') = \langle[S_i^-(t), S_j^-(t')]\rangle\delta(t-t') - \langle\langle[\mathscr{H}, S_i^-(t)]; S_j^-(t')\rangle\rangle. \tag{22}$$

Expanding the commutators, and using the Tyablikov decoupling scheme [107, 108] for higher-order functions, for example $\langle\langle S_{i'}^z S_i^+(t); S_j^-(t')\rangle\rangle \simeq \langle S_{i'}^z\rangle\langle\langle S_i^+(t); S_j^-(t')\rangle\rangle$ etc., we obtain the following general equations for non collinear magnets:

$$\begin{aligned}
\mathrm{i}\hbar\frac{\mathrm{d}G_{i,j}(t,t')}{\mathrm{d}t} = {} & 2\langle S_i^z\rangle\delta_{i,j}\delta(t-t') - \sum_{i'} J_{i,i'}\big[\langle S_i^z\rangle(\cos\theta_{i,i'} - 1)F_{i',j}(t,t') \\
& + \langle S_i^z\rangle(\cos\theta_{i,i'} + 1)G_{i',j}(t,t') - 2\langle S_{i'}^z\rangle\cos\theta_{i,i'}G_{i,j}(t,t')\big] \\
& + 2\sum_{i'} I_{i,i'}\langle S_{i'}^z\rangle\cos\theta_{i,i'}G_{i,j}(t,t')
\end{aligned} \tag{23}$$

$$i\hbar\frac{dF_{i,j}(t,t')}{dt} = \sum_{i'} J_{i,i'}\left[\langle S_i^z\rangle(\cos\theta_{i,i'}-1)G_{i',j}(t,t') + \langle S_i^z\rangle(\cos\theta_{i,i'}+1)F_{i',j}(t,t')\right.$$
$$\left. - 2\langle S_{i'}^z\rangle\cos\theta_{i,i'}F_{i,j}(t,t')\right] - 2\sum_{i'} I_{i,i'}\langle S_{i'}^z\rangle\cos\theta_{i,i'}F_{i,j}(t,t'). \quad (24)$$

In the case of a BCC thin film with a (001) surface considered here, the above equations yield a closed system of coupled equations within the Tyablikov decoupling scheme. For clarity, we separate the sums on NN interactions and NNN interactions as follows:

$$i\hbar\frac{dG_{i,j}(t,t')}{dt} = 2\langle S_i^z\rangle\delta_{i,j}\delta(t-t') - \sum_{k'\in NN} J_{i,k'}\left[\langle S_i^z\rangle(\cos\theta_{i,k'}-1)F_{k',j}(t,t')\right.$$
$$\left. + \langle S_i^z\rangle(\cos\theta_{i,k'}+1)G_{k',j}(t,t') - 2\langle S_{k'}^z\rangle\cos\theta_{i,k'}G_{i,j}(t,t')\right]$$
$$+ 2\sum_{k'\in NN} I_{i,k'}\langle S_{k'}^z\rangle\cos\theta_{i,k'}G_{i,j}(t,t') - \sum_{i'\in NNN} J_{i,i'}\left[\langle S_i^z\rangle(\cos\theta_{i,i'}-1)F_{i',j}(t,t')\right.$$
$$\left. + \langle S_i^z\rangle(\cos\theta_{i,i'}+1)G_{i',j}(t,t') - 2\langle S_{i'}^z\rangle\cos\theta_{i,i'}G_{i,j}(t,t')\right] \quad (25)$$

$$i\hbar\frac{dF_{k,j}(t,t')}{dt} = \sum_{i'\in NN} J_{k,i'}\left[\langle S_k^z\rangle(\cos\theta_{k,i'}-1)G_{i',j}(t,t')\right.$$
$$\left. + \langle S_k^z\rangle(\cos\theta_{k,i'}+1)F_{i',j}(t,t') - 2\langle S_{i'}^z\rangle\cos\theta_{k,i'}F_{k,j}(t,t')\right]$$
$$- 2\sum_{i'\in NN} I_{k,i'}\langle S_{i'}^z\rangle\cos\theta_{k,i'}F_{k,j}(t,t')$$
$$+ \sum_{k'\in NNN} J_{k,k'}\left[\langle S_k^z\rangle(\cos\theta_{k,k'}-1)G_{k',j}(t,t')\right.$$
$$\left. + \langle S_k^z\rangle(\cos\theta_{k,k'}+1)F_{k',j}(t,t') - 2\langle S_{k'}^z\rangle\cos\theta_{k,k'}F_{k,j}(t,t')\right]. \quad (26)$$

For simplicity, except otherwise stated, all NN interactions ($J_{k,k'}, I_{k,k'}$) are taken equal to (J_1, I_1) and all NNN interactions are taken equal to J_2 in the following. Furthermore, let us define the film coordinates which are used below: the c-axis is called z-axis, planes parallel to the film surface are called xy-planes and the Cartesian components of the spin position $\mathbf{R}_i$ are denoted by (ℓ_i, m_i, n_i).

We now introduce the following in-plane Fourier transforms:

$$G_{i,j}(t,t') = \frac{1}{\Delta}\int\int_{BZ} d\mathbf{k}_{xy}\frac{1}{2\pi}\int_{-\infty}^{+\infty} d\omega e^{-i\omega(t-t')} g_{n_i,n_j}(\omega,\mathbf{k}_{xy})e^{i\mathbf{k}_{xy}\cdot(\mathbf{R}_i-\mathbf{R}_j)}, \quad (27)$$

$$F_{k,j}(t,t') = \frac{1}{\Delta}\int\int_{BZ} d\mathbf{k}_{xy}\frac{1}{2\pi}\int_{-\infty}^{+\infty} d\omega e^{-i\omega(t-t')} f_{n_k,n_j}(\omega,\mathbf{k}_{xy})e^{i\mathbf{k}_{xy}\cdot(\mathbf{R}_k-\mathbf{R}_j)}, \quad (28)$$

where ω is the spin-wave frequency, $\mathbf{k}_{xy}$ denotes the wave-vector parallel to xy planes and $\mathbf{R}_i$ is the position of the spin at the site i. n_i, n_j and n_k are respectively the z-component indices of the layers where the sites $\mathbf{R}_i$, $\mathbf{R}_j$ and $\mathbf{R}_k$ belong to. The integral over $\mathbf{k}_{xy}$ is performed in the first Brillouin zone (BZ) whose surface is Δ in the xy reciprocal plane. For convenience, we denote $n_i = 1$ for all sites on the surface layer, $n_i = 2$ for all sites of the second layer and so on.

Note that for a three-dimensional case, making a 3D Fourier transformation of Equations (25)–(26) we obtain the spin-wave dispersion relation in the absence of anisotropy:

$$\hbar\omega = \pm\sqrt{A^2 - B^2} \quad (29)$$

where

$$A = J_1\langle S^z\rangle[\cos\theta + 1]Z\gamma + 2ZJ_1\langle S^z\rangle\cos\theta + J_2\langle S^z\rangle[\cos(2\theta)+1]Z_c\cos(k_z a) + 2Z_c J_2\langle S^z\rangle\cos(2\theta)$$
$$B = J_1\langle S^z\rangle(\cos\theta - 1)Z\gamma + J_2\langle S^z\rangle[\cos(2\theta)-1]Z_c\cos(k_z a)$$

where $Z = 8$ (NN number), $Z_c = 2$ (NNN number on the c-axis), $\gamma = \cos(k_x a/2)\cos(k_y a/2)\cos(k_z a/2)$ (a: lattice constant). We see that $\hbar\omega$ is zero when $A = \pm B$, namely at $k_x = k_y = k_z = 0$

($\gamma = 1$) and at $k_z = 2\theta$ along the helical axis. The case of ferromagnets (antiferromagnets) with NN interaction only is recovered by putting $\cos\theta = 1$ (-1) [92].

Let us return to the film case. We make the in-plane Fourier transformation Equations (27)–(28) for Equations (25)–(26). We obtain the following matrix equation

$$\mathbf{M}(\omega)\mathbf{h} = \mathbf{u}, \tag{30}$$

where $\mathbf{M}(\omega)$ is a square matrix of dimension $(2N_z \times 2N_z)$, $\mathbf{h}$ and $\mathbf{u}$ are the column matrices which are defined as follows

$$\mathbf{h} = \begin{pmatrix} g_{1,n'} \\ f_{1,n'} \\ \vdots \\ g_{n,n'} \\ f_{n,n'} \\ \vdots \\ g_{N_z,n'} \\ f_{N_z,n'} \end{pmatrix}, \quad \mathbf{u} = \begin{pmatrix} 2\langle S_1^z\rangle\delta_{1,n'} \\ 0 \\ \vdots \\ 2\langle S_{N_z}^z\rangle\delta_{N_z,n'} \\ 0 \end{pmatrix}, \tag{31}$$

where, taking $\hbar = 1$ hereafter,

$$\mathbf{M}(\omega) = \begin{pmatrix} \omega + A_1 & 0 & B_1^+ & C_1^+ & D_1^+ & E_1^+ & 0 & 0 & 0 & 0 & 0 & 0 \\ 0 & \omega - A_1 & -C_1^+ & -B_1^+ & -E_1^+ & -D_1^+ & 0 & 0 & 0 & 0 & 0 & 0 \\ \cdots & \cdots & \cdots & \cdots & \cdots & \cdots & \cdots & \cdots & \cdots & \cdots & \cdots & \cdots \\ \cdots & D_n^- & E_n^- & B_n^- & C_n^- & \omega + A_n & 0 & B_n^+ & C_n^+ & D_n^+ & E_n^+ & \cdots \\ \cdots & -E_n^- & -D_n^- & -C_n^- & -B_n^- & 0 & \omega - A_n & -C_n^+ & -B_n^+ & -E_n^+ & -D_n^+ & \cdots \\ \cdots & \cdots & \cdots & \cdots & \cdots & \cdots & \cdots & \cdots & \cdots & \cdots & \cdots & \cdots \\ 0 & 0 & 0 & 0 & 0 & 0 & D_{N_z}^- & E_{N_z}^- & B_{N_z}^- & C_{N_z}^- & \omega + A_{N_z} & 0 \\ 0 & 0 & 0 & 0 & 0 & 0 & -E_{N_z}^- & -D_{N_z}^- & -C_{N_z}^- & -B_{N_z}^- & 0 & \omega - A_{N_z} \end{pmatrix} \tag{32}$$

where

$$A_n = -8J_1(1+d)\left[\langle S_{n+1}^z\rangle\cos\theta_{n,n+1} + \langle S_{n-1}^z\rangle\cos\theta_{n,n-1}\right] - 2J_2\left[\langle S_{n+2}^z\rangle\cos\theta_{n,n+2} + \langle S_{n-2}^z\rangle\cos\theta_{n,n-2}\right]$$

where $n = 1, 2, \ldots, N_z$, $d = I_1/J_1$, and

$$\begin{aligned} B_n^\pm &= 4J_1\langle S_n^z\rangle(\cos\theta_{n,n\pm1} + 1)\gamma \\ C_n^\pm &= 4J_1\langle S_n^z\rangle(\cos\theta_{n,n\pm1} - 1)\gamma \\ E_n^\pm &= J_2\langle S_n^z\rangle(\cos\theta_{n,n\pm2} - 1) \\ D_n^\pm &= J_2\langle S_n^z\rangle(\cos\theta_{n,n\pm2} + 1) \end{aligned}$$

In the above expressions, $\theta_{n,n\pm1}$ the angle between a spin in the layer n and its NN spins in layers $n \pm 1$ etc. and $\gamma = \cos(k_x a/2)\cos(k_y a/2)$.

Solving $\det|\mathbf{M}| = 0$, we obtain the spin-wave spectrum ω of the present system: for each value (k_x, k_y), there are $2N_z$ eigen-values of ω corresponding to two opposite spin precessions as in antiferromagnets (the dimension of $\det|\mathbf{M}|$ is $2N_z \times 2N_z$). Note that the above equation depends on the values of $\langle S_n^z\rangle$ $(n = 1, \ldots, N_z)$. Even at temperature $T = 0$, these z-components are not equal to 1/2 because we are dealing with an antiferromagnetic system where fluctuations at $T = 0$ give rise to the so-called zero-point spin contraction [90]. Worse, in our system with the existence of the film surfaces, the spin contractions are not spatially uniform as will be seen below. So the solution of $\det|\mathbf{M}| = 0$ should be found by iteration. This will be explicitly shown hereafter.

The solution for $g_{n,n}$ is given by

$$g_{n,n}(\omega) = \frac{|\mathbf{M}|_{2n-1}}{|\mathbf{M}|}, \tag{33}$$

where $|\mathbf{M}|_{2n-1}$ is the determinant made by replacing the $2n-1$-th column of $|\mathbf{M}|$ by $\mathbf{u}$ given by Equation (31) (note that $g_{n,n}$ occupies the $(2n-1)$-th line of the matrix $\mathbf{h}$). Writing now

$$|\mathbf{M}| = \prod_i \left[\omega - \omega_i(\mathbf{k}_{xy})\right], \tag{34}$$

we see that $\omega_i(\mathbf{k}_{xy}), i = 1,\ldots, 2N_z$, are poles of $g_{n,n}$. $\omega_i(\mathbf{k}_{xy})$ can be obtained by solving $|\mathbf{M}| = 0$. In this case, $g_{n,n}$ can be expressed as

$$g_{n,n}(\omega) = \sum_i \frac{D_{2n-1}(\omega_i(\mathbf{k}_{xy}))}{\left[\omega - \omega_i(\mathbf{k}_{xy})\right]}, \tag{35}$$

where $D_{2n-1}(\omega_i(\mathbf{k}_{xy}))$ is

$$D_{2n-1}(\omega_i(\mathbf{k}_{xy})) = \frac{|\mathbf{M}|_{2n-1}(\omega_i(\mathbf{k}_{xy}))}{\prod_{j\neq i}\left[\omega_j(\mathbf{k}_{xy}) - \omega_i(\mathbf{k}_{xy})\right]}. \tag{36}$$

Next, using the spectral theorem which relates the correlation function $\langle S_i^- S_j^+\rangle$ to the Green's function [91], we have

$$\begin{aligned}\langle S_i^- S_j^+\rangle = \lim_{\varepsilon\to 0}\frac{1}{\Delta}\int\int \mathrm{d}\mathbf{k}_{xy}\int_{-\infty}^{+\infty}\frac{\mathrm{i}}{2\pi}\big(g_{n,n'}(\omega+\mathrm{i}\varepsilon)\\ - g_{n,n'}(\omega-\mathrm{i}\varepsilon)\big)\frac{\mathrm{d}\omega}{\mathrm{e}^{\beta\omega}-1}\mathrm{e}^{\mathrm{i}\mathbf{k}_{xy}\cdot(\mathbf{R}_i-\mathbf{R}_j)},\end{aligned} \tag{37}$$

where ϵ is an infinitesimal positive constant and $\beta = (k_\mathrm{B}T)^{-1}$, k_B being the Boltzmann constant.

Using the Green's function presented above, we can calculate self-consistently various physical quantities as functions of temperature T. The magnetization $\langle S_n^z\rangle$ of the n-th layer is given by

$$\begin{aligned}\langle S_n^z\rangle &= \frac{1}{2} - \langle S_n^- S_n^+\rangle\\ &= \frac{1}{2} - \lim_{\epsilon\to 0}\frac{1}{\Delta}\int\int \mathrm{d}\mathbf{k}_{xy}\int_{-\infty}^{+\infty}\frac{\mathrm{i}}{2\pi}\left[g_{n,n}(\omega+\mathrm{i}\epsilon)\right.\\ &\quad \left. - g_{n,n}(\omega-\mathrm{i}\epsilon)\right]\frac{\mathrm{d}\omega}{\mathrm{e}^{\beta\omega}-1}\end{aligned} \tag{38}$$

Replacing Equation (35) in Equation (38) and making use of the following identity

$$\frac{1}{x-\mathrm{i}\eta} - \frac{1}{x+\mathrm{i}\eta} = 2\pi\mathrm{i}\delta(x) \tag{39}$$

we obtain

$$\langle S_n^z\rangle = \frac{1}{2} - \frac{1}{\Delta}\int\int \mathrm{d}k_x\mathrm{d}k_y\sum_{i=1}^{2N_z}\frac{D_{2n-1}(\omega_i)}{\mathrm{e}^{\beta\omega_i}-1} \tag{40}$$

where $n = 1,\ldots,N_z$. As $\langle S_n^z\rangle$ depends on the magnetizations of the neighboring layers via ω_i ($i = 1,\ldots,2N_z$), we should solve by iteration the Equations (40) written for all layers, namely for $n = 1,\ldots,N_z$, to obtain the magnetizations of layers 1, 2, 3, …, N_z at a given temperature T. Note that by symmetry, $\langle S_1^z\rangle = \langle S_{N_z}^z\rangle$, $\langle S_2^z\rangle = \langle S_{N_z-1}^z\rangle$, $\langle S_3^z\rangle = \langle S_{N_z-2}^z\rangle$, and so on. Thus, only $N_z/2$ self-consistent layer magnetizations are to be calculated.

The value of the spin in the layer n at $T = 0$ is calculated by

$$\langle S_n^z\rangle(T=0) = \frac{1}{2} + \frac{1}{\Delta}\int\int \mathrm{d}k_x\mathrm{d}k_y\sum_{i=1}^{N_z} D_{2n-1}(\omega_i) \tag{41}$$

where the sum is performed over N_z negative values of ω_i (for positive values the Bose–Einstein factor is equal to 0 at $T = 0$).

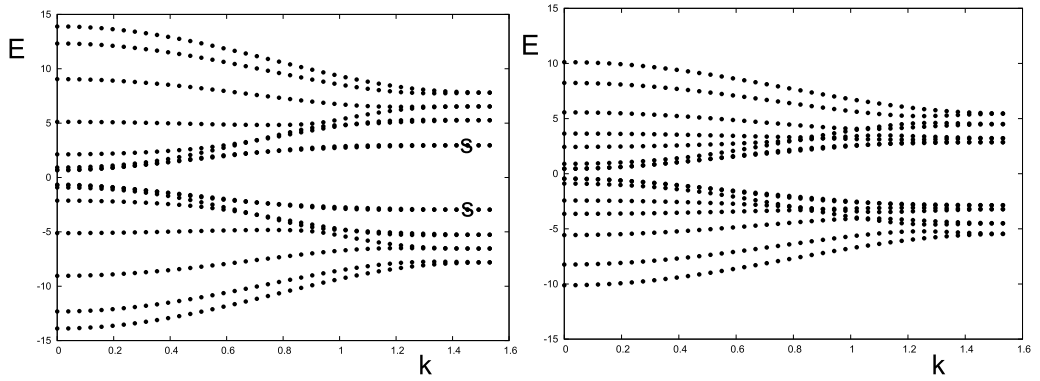

Figure 16. Spectrum $E = \hbar\omega$ versus $k \equiv k_x = k_y$ for $J_2/J_1 = -1.4$ at $T = 0.1$ (top) and $T = 1.02$ (bottom) for $N_z = 8$ and $d = 0.1$. The surface branches are indicated by s.

The transition temperature T_c can be calculated in a self-consistent manner by iteration, letting all $\langle S_n^z \rangle$ tend to zero, namely $\omega_i \to 0$. Expanding $e^{\beta\omega_i} - 1 \to \beta_c \omega_i$ on the right-hand side of Equation (40) where $\beta_c = (k_B T_c)^{-1}$, we have by putting $\langle S_n^z \rangle = 0$ on the left-hand side,

$$\beta_c = 2\frac{1}{\Delta}\int\int dk_x dk_y \sum_{i=1}^{2N_z} \frac{D_{2n-1}(\omega_i)}{\omega_i} \tag{42}$$

There are N_z such equations using Equation (40) with $n = 1, \ldots, N_z$. Since the layer magnetizations tend to zero at the transition temperature from different values, it is obvious that we have to look for a convergence of the solutions of the equations Equation (42) to a single value of T_c. The method to do this will be shown below.

Let us show the numerical results of the above equations.

6.1.1. *Spin-wave spectrum*

Figure 16 shows an example of the spin-wave spectrum ω obtained by solving $\det|\mathbf{M}| = 0$, as said above. The surface spin waves are indicated by "S" on the figure. Surface spin waves are localized on the surface and damped when going to interior layers (see explanation in [92]).

6.1.2. *Spin contraction at $T = 0$*

It is known that in antiferromagnets, quantum fluctuations give rise to a contraction of the spin length at zero temperature [90]. We will see here that a spin under a stronger antiferromagnetic interaction has a stronger zero-point spin contraction. The spins near the surface serve for such a test. In the case of the film considered above, spins in the first and in the second layers have only one antiferromagnetic NNN while interior spins have two NNN, so the contraction at a given J_2/J_1 is expected to be stronger for interior spins. This is verified with the results shown in Figure 17. When $|J_2|/J_1$ increases, namely the antiferromagnetic interaction becomes stronger, we observe stronger contractions. Note that the contraction tends to zero when the spin configuration becomes ferromagnetic, namely J_2/J_1 tends to -1.

6.1.3. *Layer magnetizations and transition temperature*

Let us show two examples of the magnetization, layer by layer, from the film surface in Figures 18 for the case where $J_2/J_1 = -1.4$ in a $N_z = 8$ film. Let us comment on these results:

(i) the shown result is obtained with a convergence of 1%. For temperatures closer to the transition temperature T_c, we have to lower the precision to a few percents which reduces the clarity because of their close values (not shown).

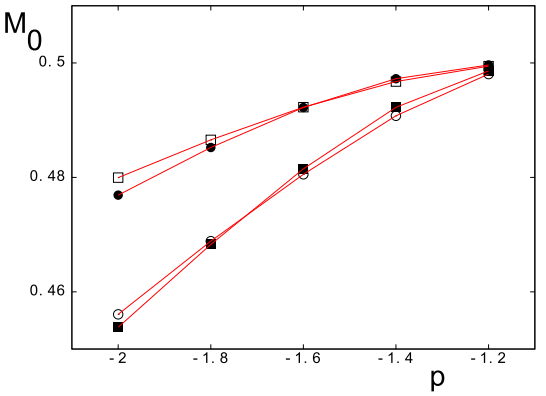

Figure 17. Spin lengths of the first four layers at $T = 0$ for several values of $p = J_2/J_1$ with $d = 0.1$, $N_z = 8$. Black circles, void circles, black squares and void squares are for first, second, third and fourth layers, respectively. See text for comments.

(ii) the surface magnetization, which has a large value at $T = 0$ as seen in Figure 17, crosses the interior layer magnetizations at $T \simeq 0.42$ to become much smaller than interior magnetizations at higher temperatures. This crossover phenomenon is due to the competition between quantum fluctuations, which dominate low-T behavior, and the low-lying surface spin-wave modes which strongly diminish the surface magnetization at higher T. Note that the second-layer magnetization makes also a crossover at $T \simeq 1.3$. Similar crossovers have been observed in quantum antiferromagnetic films [109] and quantum superlattices [110].

Note that though the layer magnetizations are different at low temperatures, they will tend to zero at a unique transition temperature as seen below. The reason is that as long as an interior layer magnetization is not zero, it will act on the surface spins as an external field, preventing them to become zero. We have calculated self-consistently the transition temperature for each value of J_2/J_1 (see [95]).

Results of other values of J_2/J_1 have been shown in [95]. Effects of d, film thickness and surface exchange interactions different from the bulk ones have been shown in that reference.

6.2. *Other applications in frustrated systems with Dzyaloshinskii–Moriya interaction*

As seen in Sections 2 and 5, non-collinear spin configurations are found in many frustrated spin systems. The Green's function technique presented above can be applied to study elementary excitations and their thermodynamic effects. We have seen above that although the formalism is rather cumbersome, the results cannot be obtained otherwise nowadays.

We have applied the above Green's function technique to study for example several systems with Dzyaloshinskii–Moriya interaction in monolayer and bilayer magneto-ferroelectric materials [82] and in antiferromagnetic triangular lattice [84]. The reader is referred to these papers for detailed results.

7. Conclusion

I have reviewed in this paper a number of personal works on the frustration effects inspired by a collaboration and numerous discussions with Gérard Toulouse, at the beginning of my career, in the early 80's. I moved in the early 90's to the new Unversity of Cergy-Pontoise. I saw him again in the years 2000 when he was a member of the Orientation Council of our university. Needless to say, I was very happy to discuss again with him on physics and on other subjects of life as well.

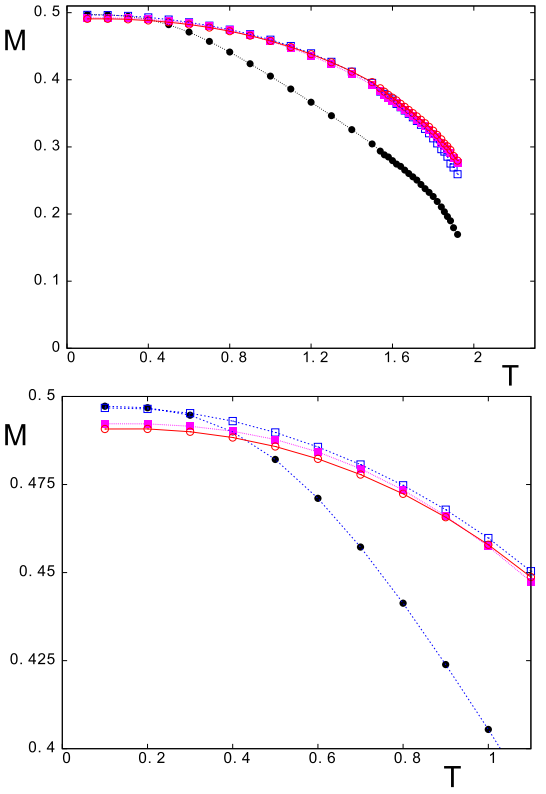

Figure 18. Layer magnetizations as functions of T for $J_2/J_1 = -1.4$ with $d = 0.1$, $N_z = 8$ (top). Zoom of the region at low T to show crossover (bottom). Black circles, blue void squares, magenta squares and red void circles are for first, second, third and fourth layers, respectively. See text.

The search for frustration effects was uninterrupted in my activities to this day. As seen in this review, frustration is at the origin of many striking phenomena, going from the coexistence of order and disorder in systems at equilibrium to the existence of reentrant phases and disorder lines, passing by systems with non-collinear spin structures and skyrmions. The frustration in materials opens many new areas of physics not only on the theoretical point of view but also on many applications in spintronics, as mentioned above. This paper is just a personal account of the emergence of a modern physics in which various frustrated systems are still actively studied.

To conclude, I would like to emphasize that the concept of frustration is found also in other disciplines such as biology [111] where geometric frustration can drive the development of structure in complex biological systems, and may have implications for the nature of the actin-myosin interactions involved in muscle contraction. In chemistry, the so-called "chemical frustration" allows to explain chemical properties of many complex compounds [112, 113]. Even in sociophysics where individuals are represented by spins, the frustration due to conflicts plays an important role in the dynamics of social groups [114, 115].

Declaration of interests

The authors do not work for, advise, own shares in, or receive funds from any organization that could benefit from this article, and have declared no affiliations other than their research organizations.

Acknowledgments

The author is grateful to his many collaborators and former doctorate students for contributions to works mentioned in this paper.

References

[1] G. Toulouse, "Theory of frustration effects in spin glass: I", *Commun. Phys.* **2** (1977), pp. 115–119.
[2] J. Villain, "Spin glass with non-random interactions", *J. Phys. C* **10** (1977), pp. 1717–1734.
[3] K. G. Wilson, "Renormalization group and critical phenomena. I. Renormalization group and the Kadanoff scaling picture", *Phys. Rev. B* **4** (1971), pp. 3174–3183.
[4] D. J. Amit, *Field Theory, The Renormalization Group and Critical Phenomena*, World Scientific: Singapore, 1984.
[5] J. Cardy, *Scaling and Renormalization in Statistical Physics*, Cambridge University Press: London, 1996.
[6] J. Zinn-Justin, *Quantum Field Theory and Critical Phenomena*, 4th edition, Oxford University Press: London, 2002.
[7] R. J. Baxter, *Exactly Solved Models in Statistical Mechanics*, Academic: New York, 1982.
[8] A. Yoshimori, "A new type of antiferromagnetic structure in the rutile type crystal", *J. Phys. Soc. Jpn* **14** (1959), pp. 807–821.
[9] J. Villain, "La structure des substances magnetiques", *Phys. Chem. Solids* **11** (1959), pp. 303–330.
[10] G. H. Wannier, "Antiferromagnetism. The triangular Ising net", *Phys. Rev.* **79** (1950), pp. 357–364.
[11] G. H. Wannier, "Antiferromagnetism. The triangular Ising net", *Phys. Rev. B* **7** (1973), p. 5017. (Erratum).
[12] H. Kawamura, "Renormalization-group analysis of chiral transitions", *Phys. Rev. B* **38** (1988), pp. 4916–4928. Erratum *Phys. Rev. B*, **42**, 1990, 2610.
[13] H. Kawamura, "Universality of phase transitions of frustrated antiferromagnets", *J. Phys. Condens. Matter* **10** (1998), pp. 4707–4754.
[14] B. Delamotte, D. Mouhanna and M. Tissier, "Nonperturbative renormalization group approach to frustrated magnets", *Phys. Rev. B* **69** (2004), article no. 134413.
[15] B. Delamotte, M. Dudka, Y. Holovatch and D. Mouhanna, "About the relevance of the fixed dimension perturbative approach to frustrated magnets in two and three dimensions", *Phys. Rev. B* **82** (2010), article no. 104432.
[16] M. Reehorst, S. Rychkov, B. Sirois and B. C. van Rees, *Bootstrapping frustrated magnets: the fate of the chiral O(N) × O(2) universality class*, preprint, 2024, 2405.19411v2.
[17] C. A. Sánchez-Villalobos, B. Delamotte and N. Wschebor, *O(N) × O(2) scalar models: including O(∂2) corrections in the Functional Renormalization Group analysis*, preprint, 2024, 2411.02616v1.
[18] V.-T. Ngo and H. T. Diep, "Phase transition in Heisenberg stacked triangular antiferromagnets: End of a controversy", *Phys. Rev. E* **78** (2008), article no. 031119.
[19] V.-T. Ngo and H. T. Diep, "Stacked triangular XY antiferromagnets: End of a controversial issue on the phase transition", *J. Appl. Phys.* **103** (2008), article no. 07C712.
[20] P. Lallemand, H. T. Diep, A. Ghazali and G. Toulouse, "Configuration space analysis for fully frustrated vector spins", *J. Phys. Lett.* **46** (1985), pp. 1087–1093.
[21] H. T. Diep, P. Lallemand and O. Nagai, "Simple cubic fully frustrated Ising crystal by Monte Carlo simulations", *J. Appl. Phys.* **57** (1985), pp. 3309–3311.
[22] H. T. Diep, A. Ghazali and P. Lallemand, "A fully frustrated simple cubic lattice with XY and Heisenberg spin : ground state and phase transition", *J. Phys. C* **18** (1985), pp. 5881–5895.
[23] B. Derrida, Y. Pomeau, G. Toulouse and J. Vannimenus, "Fully frustrated simple cubic lattices and the overblocking effect", *J. Physique* **40** (1979), pp. 617–626.
[24] B. Derrida, Y. Pomeau, G. Toulouse and J. Vannimenus, "Fully frustrated simple cubic lattices and phase transitions", *J. Physique* **41** (1980), pp. 213–221.
[25] *Frustrated Spin Systems*, 3rd edition (H. T. Diep, ed.), World Scientific: Singapore, 2020.
[26] P. Duwez, R. H. Willens and W. Klement Jr, "Continuous series of metastable solid solutions of silver-copper alloys", *J Appl. Phys.* **31** (1960), pp. 1136–1137.
[27] *Rapidly Quenched Metals*, 1st edition (S. Steeb, ed.), Elsevier: Amsterdam, 2012. Note: The reviews of this book were papers presented at the Fifth International Conference on Rapidly Quenched Metals, held in Wurzburg, Germany on September 3–7, 1984.
[28] S. F. Edwards and P. W. Anderson, "Theory of spin glasses", *J. Phys. F: Metal Phys.* **5** (1975), no. 5, pp. 965–974.
[29] D. Sherrington and S. Kirkpatrick, "Solvable model of a spin-glass", *Phys. Rev. Lett.* **35** (1975), no. 26, pp. 1792–1796.
[30] G. Parisi, "Infinite number of order parameters for spin-glasses", *Phys. Rev. Lett.* **43** (1979), no. 23, pp. 1754–1756.
[31] M. Mézard, G. Parisi and M. A. Virasoro, *Spin Glass Theory and Beyond*, World Scientific: Singapore, 1987.

[32] O. Nagai, M. Toyonaga and H. T. Diep, "Effect of bond disorder in the Ising spin glass problem", *J. Magn. Magn. Mater.* **31–34** (1983), pp. 1313–1314.
[33] H. T. Diep and O. Nagai, "Monte Carlo study of a three-dimensional Ising lattice with frustration", *J. Phys. C: Solid State Phys.* **17** (1984), pp. 1357–1365.
[34] A. Ghazali, P. Lallemand and H. T. Diep, "Spin-glass transition in Heisenberg spin system with ±J random bonds", *Physica A* **134** (1986), pp. 628–635.
[35] A. T. Ogielski, "Dynamics of three-dimensional Ising spin glasses in thermal equilibrium", *Phys. Rev. B* **32** (1985), pp. 7384–7398.
[36] H. T. Diep, "First-order transition in the hexagonal-close-packed lattice with vector spins", *Phys. Rev. B* **45** (1992), pp. 2863–2867.
[37] D.-T. Hoang and H. T. Diep, "Hexagonal-close-packed lattice: ground state and phase transition", *Phys. Rev. E* **85** (2012), article no. 041107.
[38] H. T. Diep and H. Kawamura, "First-order transition in the FCC Heisenberg antiferromagnet", *Phys. Rev. B* **40** (1989), pp. 7019–7022.
[39] H. T. Diep and H. Giacomini, "Frustration—exactly solved models", in *Frustrated Spin Systems*, 3rd edition (H. T. Diep, ed.), World Scientific: Singapore, 2020.
[40] B. Berge, H. T. Diep, A. Ghazali and P. Lallemand, "Phase transitions in two-dimensional uniformly frustrated XY spin systems", *Phys. Rev. B* **34** (1986), pp. 3177–3184.
[41] I. Harada and K. Motizuki, "Effect of magnon-magnon interaction on spin wave dispersion and magnon sideband in MnS", *J. Phys. Soc. Jpn* **32** (1972), pp. 927–940.
[42] E. Rastelli, L. Reatto and A. Tassi, "Quantum fluctuations in helimagnets", *J. Phys. C* **18** (1985), pp. 353–360.
[43] H. T. Diep, "Low-temperature properties of quantum Heisenberg helimagnets", *Phys. Rev. B* **40** (1989), pp. 741–744.
[44] P. Azaria, H. T. Diep and H. Giacomini, "Coexistence of order and disorder and reentrance in an exactly solvable model", *Phys. Rev. Lett.* **59** (1987), pp. 1629–1632.
[45] M. Debauche, H. T. Diep, P. Azaria and H. Giacomini, "Exact phase diagram in a generalized Kagomé Ising lattice: reentrance and disorder lines", *Phys. Rev. B* **44** (1991), pp. 2369–2372.
[46] H. T. Diep, M. Debauche and H. Giacomini, "Exact solution of an anisotropic centered honeycomb Ising lattice: Reentrance and Partial Disorder", *Phys. Rev. B* **43** (1991), pp. 8759–8762. (Rapid Communication).
[47] M. Debauche and H. T. Diep, "Successive reentrances and phase transitions in exactly solved dilute centered square ising lattices", *Phys. Rev. B* **46** (1992), pp. 8214–8218.
[48] H. T. Diep, M. Debauche and H. Giacomini, "Reentrance and disorder solutions in exactly solvable ising models", *J. Magn. Magn. Mater.* **104** (1992), pp. 184–186.
[49] V. Vaks, A. Larkin and Y. Ovchinnikov, "Ising model with interaction between nonnearest neighbors", *Sov. Phys. JEPT* **22** (1966), pp. 820–826.
[50] K. Kano and S. Naya, "Antiferromagnetism. The Kagomé Ising net", *Prog. Theor. Phys.* **10** (1953), pp. 158–172.
[51] J. Stephenson, "Ising-model spin correlations on the triangular lattice. IV. Anisotropic ferromagnetic and antiferromagnetic lattices", *J. Math. Phys.* **11** (1970), pp. 420–431.
[52] J. Stephenson, "Range of order in antiferromagnets with next-nearest neighbor coupling", *Can. J. Phys.* **48** (1970), pp. 2118–2122.
[53] J. Stephenson, "Ising model with antiferromagnetic next-nearest-neighbor coupling: Spin correlations and disorder points", *Phys. Rev. B* **1** (1970), pp. 4405–4409.
[54] R. Quartu and H. T. Diep, "Partial order in frustrated quantum spin systems", *Phys. Rev. B* **55** (1997), pp. 2975–2980.
[55] C. Santamaria and H. T. Diep, "Evidence of a partial disorder in a frustrated Heisenberg system", *J. Appl. Phys.* **81** (1997), pp. 5276–5278.
[56] E. H. Boubcheur, R. Quartu, H. T. Diep and O. Nagai, "Non collinear XY spin system: first-order transition and evidence of a reentrance", *Phys. Rev. B* **58** (1998), pp. 400–408.
[57] F. Wang and D. P. Landau, "Efficient, multiple-range random walk algorithm to calculate the density of states", *Phys. Rev. Lett.* **86** (2001), pp. 2050–2053.
[58] F. Wang and D. P. Landau, "Determining the density of states for classical statistical models", *Phys. Rev. E* **64** (2001), article no. 056101.
[59] G. Brown and T. C. Schulhess, "Wang–Landau estimation of magnetic properties for the Heisenberg model", *J. Appl. Phys.* **97** (2005), article no. 10E303.
[60] B. J. Schulz, K. Binder, M. Müller and D. P. Landau, "Avoiding boundary effects in Wang–Landau sampling", *Phys. Rev. E* **67** (2003), article no. 067102.
[61] A. Malakis, S. S. Martinos, I. A. Hadjiagapiou, N. G. Fytas and P. Kalozoumis, "Entropic sampling via Wang–Landau random walks in dominant energy subspaces", *Phys. Rev. E* **72** (2005), article no. 066120.

[62] V.-T. Ngo, D. T. Hoang and H. T. Diep, "First-order transition in XY fully frustrated simple cubic lattice", *Phys. Rev. E* **82** (2010), article no. 041123.

[63] V. T. Ngo, D. T. Hoang and H. T. Diep, "Phase transition in heisenberg fully frustrated simple cubic lattice", *Mod. Phys. Lett. B* **25** (2011), pp. 929–936.

[64] C. Pinettes and H. T. Diep, "Phase transition and phase diagram of the J1–J2 Heisenberg model on a simple cubic lattice", *J. Appl. Phys.* **83** (1998), pp. 6317–6319.

[65] D. T. Hoang, Y. Magnin and H. T. Diep, "Spin resistivity in the frustrated J1–J2 model", *Mod. Phys. Lett. B* **25** (2011), pp. 937–945.

[66] E. H. Boubcheur and H. T. Diep, "Critical behavior of the two-dimensional fully frustrated XY model", *Phys. Rev. B* **58** (1998), pp. 5163–5165.

[67] M. P. Nightingale, E. Granato and J. M. Kosterlitz, "Conformal anomaly and critical exponents of the XY Ising model", *Phys. Rev. B* **52** (1995), pp. 7402–7411.

[68] E. Granato and M. P. Nightingale, "Chiral exponents of the square-lattice frustrated XY model: a Monte Carlo transfer-matrix calculation", *Phys. Rev. B* **48** (1993), pp. 7438–7444.

[69] J. Lee, J. M. Kosterlitz and E. Granato, "Monte Carlo study of frustrated *XY* models on a triangular and square lattice", *Phys. Rev. B* **43** (1991), pp. 11531–11534.

[70] E. Granato, J. M. Kosterlitz, J. Lee and M. P. Nightingale, "Phase transitions in coupled XY-Ising systems", *Phys. Rev. Lett.* **66** (1991), pp. 1090–1093.

[71] A. N. Bogdanov, U. K. Rößler and A. A. Shestakov, "Skyrmions in liquid crystals", *Phys. Rev. E* **67** (2003), article no. 016602.

[72] A. Fert, V. Cros and J. Sampaio, "Skyrmions on the track", *Nat. Nanotechnol.* **8** (2013), pp. 152–156.

[73] A. O. Leonov, I. E. Dragumov, U. K. Rößler and A. N. Bogdanov, "Theory of skyrmion states in liquid crystals", *Phys. Rev. E* **90** (2014), article no. 042502.

[74] M. Ezawa, "Giant skyrmions stabilized by dipole–dipole interactions in thin ferromagnetic films", *Phys. Rev. Lett.* **105** (2010), article no. 197202.

[75] X. C. Zhang, M. Ezawa and Y. Zhou, "Magnetic skyrmion logic gates: conversion, duplication and merging of skyrmions", *Sci. Rep.* **5** (2015), article no. 9400.

[76] X. C. Zhang, J. Xia, Y. Zhou, X. Liu, H. Zhang and M. Ezawa, "Skyrmion dynamics in a frustrated ferromagnetic film and current-induced helicity locking-unlocking transition", *Nat. Commun.* **8** (2017), article no. 1717.

[77] J. Xia et al., "Current-driven skyrmionium in a frustrated magnetic system", *Appl. Phys. Lett.* **117** (2020), article no. 012403.

[78] X. C. Zhang, J. Xia, M. Ezawa, O. A. Tretiakov, H. T. Diep, G. Zhao, X. Liu and Y. Zhou, "A frustrated bimeronium: static structure and dynamics", *Appl. Phys. Lett.* **118** (2021), article no. 052411.

[79] T. Okubo, S. Chung and H. Kawamura, "Multiple-states and the skyrmion lattice of the triangular-lattice Heisenberg antiferromagnet under magnetic fields", *Phys. Rev. Lett.* **108** (2012), article no. 017206.

[80] S. Hayami, S. Z. Lin and C. D. Batista, "Bubble and skyrmion crystals in frustrated magnets with easy-axis anisotropy", *Phys. Rev. B* **93** (2016), article no. 184413.

[81] S. El Hog, A. Bailly-Reyre and H. T. Diep, "Stability and phase transition of skyrmion crystals generated by Dzyaloshinskii-Moriya interaction", *J. Magn. Magn. Mater.* **455** (2018), pp. 32–38.

[82] I. F. Sharafullin, M. K. Kharrasov and H. T. Diep, "Dzyaloshinskii-Moriya interaction in magneto-ferroelectric superlattices: Spin waves and skyrmions", *Phys. Rev. B* **99** (2019), article no. 214420.

[83] I. Sharafullin and H. T. Diep, "Skyrmion crystals and phase transitions in Magneto-Ferroelectric superlattices: Dzyaloshinskii–Moriya interaction in a frustrated $J_1 - J_2$ model", *Symmetry* **12** (2020), pp. 26–41.

[84] S. El Hog, I. F. Sharafullin, H. T. Diep, H. Garbouj, M. Debbichi and M. Said, "Frustrated antiferromagnetic triangular lattice with Dzyaloshinskii–Moriya interaction: Ground states, spin waves, skyrmion crystal, phase transition", *J. Magn. Magn. Mater.* **563** (2022), article no. 169920. and references therein.

[85] W. Kang, Y. Huang, X. Zhang, Y. Zhou and W. Zhao, "Skyrmion-electronics: an overview and outlook", *Proc. IEEE* **104** (2016), no. 10, pp. 1–22.

[86] H. D. Rosales, D. C. Cabra and P. Pujol, "Three-sublattice Skyrmions crystal in the antiferromagnetic triangular lattice", *Phys. Rev. B* **92** (2015), article no. 214439.

[87] M. Mohylna and M. Žukovič, "Stability of skyrmion crystal phase in antiferromagnetic triangular lattice with DMI and single-ion anisotropy", *J. Magn. Magn. Mater.* **546** (2022), article no. 168840.

[88] M. Mohylna et al., "Formation and growth of skyrmion crystal phase in a frustrated Heisenberg antiferromagnet with Dzyaloshinskii-Moriya interaction", *J. Magn. Magn. Mater.* **527** (2021), article no. 167755.

[89] Z. Liu, M. d. S. Dias and S. Lounis, "Theoretical investigation of antiferromagnetic skyrmions in a triangular monolayer", *J. Phys.: Condens. Matter* **32** (2020), article no. 425801.

[90] H. T. Diep, *Theory of Magnetism — Applications to Surface Physics*, World Scientific: Singapore, 2014.

[91] D. N. Zubarev, "Double-time green functions in statistical physics", *Sov. Phys. Uspekhi* **3** (1960), pp. 320–345.

[92] H. T. Diep, J. C. S. Levy and O. Nagai, "Effects of surface spin waves and surface anisotropy in magnetic thin films at finite temperatures", *Phys. Status Solidi (b)* **93** (1979), pp. 351–361.
[93] V. Thanh Ngo and H. T. Diep, "Frustration effects in antiferromagnetic face-centered cubic Heisenberg films", *J. Phys.: Condens. Matter* **19** (2007), article no. 386202.
[94] V. T. Ngo and H. T. Diep, "Effects of frustrated surface in Heisenberg thin films", *Phys. Rev. B* **75** (2007), article no. 035412.
[95] H. T. Diep, "Quantum theory of helimagnetic thin films", *Phys. Rev. B* **91** (2015), article no. 014436.
[96] *Ultrathin Magnetic Structures*, (J. A. C. Bland and B. Heinrich, eds.), Springer-Verlag: Berlin, 1994.
[97] A. Zangwill, *Physics at Surfaces*, Cambridge University: Cambridge, 1988.
[98] V. D. Mello, C. V. Chianca, A. L. Danta and A. S. Carriço, "Magnetic surface phase of thin helimagnetic films", *Phys. Rev. B* **67** (2003), article no. 012401.
[99] F. Cinti, A. Cuccoli and A. Rettori, "Exotic magnetic structures in ultrathin helimagnetic holmium films", *Phys. Rev. B* **78** (2008), article no. 020402(R).
[100] L. J. Rodrigues, V. D. Mello, D. H. A. L. Anselmo and M. S. Vasconcelos, "Magnetic structures in ultra-thin Holmium films: Influence of external magnetic field", *J. Magn. Magn. Mater.* **377** (2015), pp. 24–28.
[101] E. A. Karhu, S. Kahwaji, M. D. Robertson, H. Fritzsche, B. J. Kirby, C. F. Majkrzak and T. L. Monchesky, "Helical magnetic order in MnSi thin films", *Phys. Rev. B* **84** (2011), article no. 060404(R).
[102] E. A. Karhu et al., "Chiral modulation and reorientation effects in MnSi thin films", *Phys. Rev. B* **85** (2012), article no. 094429.
[103] J. Heurich, J. König and A. H. MacDonald, "Persistent spin currents in helimagnets", *Phys. Rev. B* **68** (2003), article no. 064406.
[104] O. Wessely, B. Skubic and L. Nordstrom, "Spin-transfer torque in helical spin-density waves", *Phys. Rev. B* **79** (2009), article no. 104433.
[105] F. Jonietz, S. Mühlbauer, C. Pfleiderer, et al., "Spin transfer torques in MnSi at ultralow current densities", *Science* **330** (2010), pp. 1648–1651.
[106] N. D. Mermin and H. Wagner, "Absence of ferromagnetism or antiferromagnetism in one-or two-dimensional isotropic Heisenberg models", *Phys. Rev. Lett.* **17** (1966), pp. 1133–1136.
[107] S. V. Tyablikov, "Retarded and advanced Green functions in the theory of ferromagnetism", *Ukr. Mat. Zh.* **11** (1959), pp. 287–289.
[108] S. V. Tyablikov, *Methods in the Quantum Theory of Magnetism*, Plenum Press: New York, 1967.
[109] H. T. Diep, "Quantum effects in antiferromagnetic thin films", *Phys. Rev. B* **43** (1991), pp. 8509–8515.
[110] H. T. Diep, "Theory of antiferromagnetic superlattices at finite temperatures", *Phys. Rev. B* **40** (1989), pp. 4818–4823.
[111] R. P. Millane, D. H. Wojtas, C. H. Yoon, et al., "Geometric frustration in the myosin superlattice of vertebrate muscle", *J. R. Soc. Interface* **18** (2021), article no. 20210585.
[112] D. C. Fredrickson, "Electronic packing frustration in complex intermetallic structures: the role of chemical pressure in Ca_2Ag_7", *J. Am. Chem. Soc.* **133** (2011), pp. 10070–10073.
[113] N. A. Harris, A. B. Hadler and D. C. Fredrickson, "In search of chemical frustration in the Ca–Cu–Cd system: chemical pressure relief in the crystal structures of Ca_5Cu_2Cd and $Ca_2Cu_2Cd_9$", *Z. Anorg. Allg. Chem.* **637** (2011), pp. 1961–1974.
[114] G. G. Naumis, F. Samaniego-Steta, M. del Castillo-Mussot and G. J. Vázquez, "Three-body interactions in sociophysics and their role in coalition forming", *Physica A* **379** (2007), pp. 226–234.
[115] M. Kaufman, H. T. Diep and S. Kaufman, "Sociophysics of intractable conflicts: three-group dynamics", *Physica A* **517** (2019), pp. 175–187.